Reduced order models for a two-dimensional heat diffusion system.

Bharath Bhikkaji*, Kaushik Mahata*, Torsten Söderström*

April 9, 2003

Abstract

In this paper, a two-dimensional heat diffusion system, which is modeled by a partial differential equation (PDE) is considered. Finite order approximations, for the infinite order PDE model, are constructed first by a direct application of the standard finite difference approximation (FD) scheme. Using tools of linear algebra, the constructed FD approximate models are reduced to computationally simpler models without any loss of accuracy. Further, the reduced approximate models are modified by replacing its poles with their respective asymptotic limits. Numerical experiments suggest that the proposed modifications improve the accuracy of the approximate models.

Keywords: Diffusion, State-space model, Finite difference, Model reduction, Eigen-values and Eigen-vectors.

*Systems and Control Group, Department of Information Technology, Uppsala University, P O Box 337, SE 75121, Uppsala, Sweden, email bb@it.uu.se, km@it.uu.se, ts@it.uu.se

1 Introduction

Diffusion is a phenomenon in which particles disperse from regions of higher density to regions of lower density. Many physical processes, like flow of chemicals across a concentration gradient, see [19], dynamics of short rates in a stock market, see [13], flow of heat across a temperature gradient, see [1], are known to involve diffusion phenomena. Recently, diffusion systems have thrown a lot of interest among control engineers both due to its practical importance and also due to the existence of precise mathematical models governing a diffusion system, see [2], [5], [6], [11], [12] and [19].

Diffusion systems are normally modeled by PDE's, see [16]. Since PDE's are infinite order dynamic systems, any attempt to simulate the dynamics of a diffusion system would involve approximating the infinite order PDE by a finite order model. Therefore, constructing a finite order approximation for the PDE governing the diffusion system is an important task one has to undertake, while dealing with diffusion systems.

Here, we consider a special case of a two-dimensional heat diffusion across a homogeneous rectangular surface. The heat diffusion system considered here is similar to the ones mentioned in [2], [12] and references therein. In [2] and [12] the authors have considered a two-dimensional diffusion system, which is modeled by a PDE with appropriate boundary conditions. In an attempt to simulate the diffusion system, the authors in [2] and [12] have approximated the PDE model by a direct application of the standard FD approximation scheme, see [8]. In this paper, we take a system theoretic approach to construct approximate models for the chosen diffusion system. The approximate models constructed here are computationally less burdensome than the ones obtained by a direct application of the FD approximation. Further, simulations indicate that they are also more accurate than the ones obtained by using FD approximation.

In this paper, we first convert the given PDE model of the chosen diffusion system, into a linear time-invariant (LTI) system with an infinite order transfer-function. We then construct finite order approximations of the infinite order transfer-function, first using the standard FD approximation scheme. Then, by using simple tools of linear algebra, we obtain a realization of the constructed FD approximation, which has the same input-output response as the FD approximate model but has much smaller computational complexity than the original FD approximation. The convergence analysis of the FD approximation yields the asymptotic limits of its poles. Using these asymptotic limits we modify the FD approximation, by replacing the poles with their respective asymptotic limits. Simulations suggest that these modifications improve the accuracy of the FD approximations significantly.

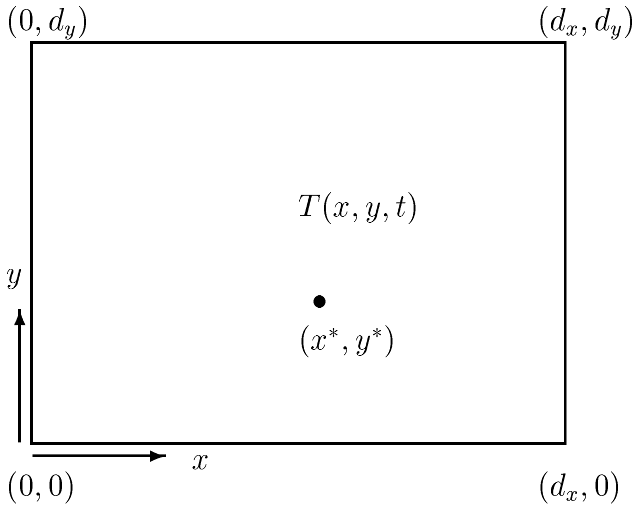

Figure 1: Heat diffusion across a two-dimensional planar region.

2 Problem description

Consider a homogeneous two-dimensional rectangular region, see Figure 1, $\Omega = [0, d_x] \times [0, d_y]$. Let the boundaries of the rectangular region corresponding to $y = 0$ and $x = d_x$ be insulated, and the boundaries corresponding to $x = 0$ and $y = d_y$ be supplied with heat $q_1(t)$ and $q_2(t)$ respectively. Let $T(x, y, t)$ denote the temperature at the point (x, y) at time t.

The dynamics of the temperature $T(x, y, t)$ is governed by the PDE

$$\frac{\partial T(x,y,t)}{\partial t} = \frac{\partial^2 T(x,y,t)}{\partial x^2} + \frac{\partial^2 T(x,y,t)}{\partial y^2} \quad (x,y) \in \Omega \tag{1}$$

with boundary conditions

$$-\frac{\partial T(x,y,t)}{\partial x}\Big|_{x=0} = q_1(t) \quad 0 \le y \le d_y, \tag{2}$$

$$\frac{\partial T(x,y,t)}{\partial y}\Big|_{y=0} = 0 \quad 0 \le x \le d_x, \tag{3}$$

$$\frac{\partial T(x,y,t)}{\partial x}\Big|_{x=d_x} = 0 \quad 0 \le y \le d_y, \tag{4}$$

and

$$-\frac{\partial T(x,y,t)}{\partial y}\Big|_{y=d_y} = q_2(t) \quad 0 \le x \le d_x, \tag{5}$$

for all $t > 0$. For the sake of brevity we assume the initial condition to be

$$T(x, y, 0) = 0 \quad (x, y) \in \Omega. \tag{6}$$

It is known that PDE's are infinite order dynamic systems. In the next section, we will show that the given PDE, (1)-(6), is an LTI system with an infinite order transfer-function. Therefore, to numerically compute the solution $T(x, y, t)$ of the given PDE, at any desired point (x, y) in Ω, one has to approximate the infinite order dynamics of the PDE by a finite order model. In this paper, we consider the problem of constructing effective finite order approximations for the chosen PDE, to compute the temperature $T(x^*, y^*, t)$ at a desired point $(x^*, y^*) \in \Omega$, given the boundary data $q_1(t)$ and $q_2(t)$. The choice of the desired point (x^*, y^*), see Figure 1, is arbitrary and has no physical significance.

3 System dynamics

In this section, we transform the given PDE model (1)-(6) into an LTI system with boundary data $q_1(t)$ and $q_2(t)$ as input and the desired temperature $T(x^*, y^*, t)$ as the output.

Taking Laplace transforms on both sides of the PDE, we get

$$s\mathcal{T}(x, y, s) = \frac{\partial^2 \mathcal{T}(x, y, s)}{\partial x^2} + \frac{\partial^2 \mathcal{T}(x, y, s)}{\partial y^2} \quad (x, y) \in \Omega, \tag{7}$$

where s is the Laplace variable and $\mathcal{T}(x, y, s)$ is the Laplace transform of $T(x, y, t)$. Similarly, taking the Laplace transforms of the boundary conditions, (2)-(5), gives

$$\begin{aligned}
-\frac{\partial \mathcal{T}(x, y, s)}{\partial x}\Big|_{x=0} &= q_1(s) \quad 0 \le y \le d_y, && (8)\\
\frac{\partial \mathcal{T}(x, y, s)}{\partial y}\Big|_{y=0} &= 0 \quad 0 \le x \le d_x, && (9)\\
\frac{\partial \mathcal{T}(x, y, s)}{\partial x}\Big|_{x=d_x} &= 0 \quad 0 \le y \le d_y && (10)\\
-\frac{\partial \mathcal{T}(x, y, s)}{\partial y}\Big|_{y=d_y} &= q_2(s) \quad 0 \le x \le d_x, && (11)
\end{aligned}$$

where $q_1(s)$ and $q_2(s)$ are Laplace transforms of $q_1(t)$ and $q_2(t)$, respectively.

It can be checked that the transformed PDE (7) has a solution of the form

$$\begin{aligned}
\mathcal{T}(x, y, s) &= A(s)\sinh(x\sqrt{s}) + B(s)\cosh(x\sqrt{s}) \\
&+ C(s)\sinh(y\sqrt{s}) + D(s)\cosh(y\sqrt{s}), && (12)
\end{aligned}$$

where the 'coefficients' $A(s)$, $B(s)$, $C(s)$ and $D(s)$ are determined by the boundary conditions (8)-(11).

Note that differentiating $\mathcal{T}(x,y,s)$, (12), with respect to x and y gives

$$\frac{\partial \mathcal{T}(x,y,s)}{\partial x} = \sqrt{s}\left(A(s)\cosh(x\sqrt{s}) + B(s)\sinh(x\sqrt{s})\right) \tag{13}$$

and

$$\frac{\partial \mathcal{T}(x,y,s)}{\partial y} = \sqrt{s}\left(C(s)\cosh(y\sqrt{s}) + D(s)\sinh(y\sqrt{s})\right). \tag{14}$$

Hence, using (13) in (8), we get

$$A(s) = -\frac{q_1(s)}{\sqrt{s}}, \tag{15}$$

and using (14) in (9), we get

$$C(s) = 0. \tag{16}$$

Similarly, using (13) and (14) in (10) and (11), respectively, we get

$$B(s) = \frac{q_1(s)}{\sqrt{s}}\coth(d_x\sqrt{s}) \tag{17}$$

and

$$D(s) = -\frac{q_2(s)}{\sqrt{s}\sinh(d_y\sqrt{s})}. \tag{18}$$

Therefore from (12), (15), (16), (17) and (18), we have

$$\begin{aligned}
\mathcal{T}(x,y,s) &= -\frac{q_1(s)}{\sqrt{s}}\sinh(x\sqrt{s}) + \frac{q_1(s)}{\sqrt{s}}\coth(d_x\sqrt{s})\cosh(x\sqrt{s}) \\
&- \frac{q_2(s)}{\sqrt{s}\sinh(d_y\sqrt{s})}\cosh(y\sqrt{s}) \\
&= \left[\begin{array}{cc} -\frac{\sinh(x\sqrt{s})}{\sqrt{s}} + \frac{\coth(d_x\sqrt{s})\cosh(x\sqrt{s})}{\sqrt{s}} & \frac{\cosh(y\sqrt{s})}{\sqrt{s}\sinh(d_y\sqrt{s})} \end{array}\right] \\
&\quad \times \left[\begin{array}{c} q_1(s) \\ q_2(s) \end{array}\right].
\end{aligned} \tag{19}$$

Since

$$\begin{aligned}
-\sinh(x\sqrt{s}) + \coth(d_x\sqrt{s})\cosh(x\sqrt{s}) &= -\sinh(x\sqrt{s}) \\
&\quad + \frac{\cosh(d_x\sqrt{s})\cosh(x\sqrt{s})}{\sinh(d_x\sqrt{s})} \\
&= \left(\frac{\cosh(d_x\sqrt{s})\cosh(x\sqrt{s})}{\sinh(d_x\sqrt{s})}\right. \\
&\quad \left. - \frac{\sinh(d_x\sqrt{s})\sinh(x\sqrt{s})}{\sinh(d_x\sqrt{s})}\right) \\
&= \frac{\cosh((d_x - x)\sqrt{s})}{\sinh(d_x\sqrt{s})}, \qquad (20)
\end{aligned}$$

(19) can be re-written as

$$\mathcal{T}(x, y, s) = \left[\begin{array}{cc} \frac{\cosh((d_x - x)\sqrt{s})}{\sqrt{s}\sinh(d_x\sqrt{s})} & \frac{\cosh(y\sqrt{s})}{\sqrt{s}\sinh(d_y\sqrt{s})} \end{array} \right] \left[\begin{array}{c} q_1(s) \\ q_2(s) \end{array} \right]. \qquad (21)$$

Replacing the general co-ordinates (x, y) by the desired co-ordinates (x^*, y^*) in (21), we have an LTI system with

$$\begin{aligned}
G(s) &= \left[\begin{array}{cc} \frac{\cosh((d_x - x^*)\sqrt{s})}{\sqrt{s}\sinh(d_x\sqrt{s})} & \frac{\cosh(y^*\sqrt{s})}{\sqrt{s}\sinh(d_y\sqrt{s})} \end{array} \right] \\
&\triangleq [G_1(s)\ G_2(s)], \qquad (22)
\end{aligned}$$

as the transfer-function, the boundary data $q_1(t)$ and $q_2(t)$ as the input, and the temperature $T(x^*, y^*, t)$ as the output.

Since $G_1(s)$ and $G_2(s)$ are transcendental functions, (21) is an LTI system with an infinite order transfer-function. In most applications involving LTI systems, one would prefer to have a rational transfer-function, or a finite order transfer-function, over a transcendental transfer-function, as it is much simpler to implement a rational transfer-function using most standard simulation tools. Therefore, approximating the infinite order dynamics of the chosen heat diffusion system can also be interpreted as constructing rational approximations for the transcendental transfer-functions $G_1(s)$ and $G_2(s)$.

Note that $G_1(s)$ is independent of the y co-ordinate and $G_2(s)$ is independent of the x co-ordinate, hence, the chosen diffusion system, (21), is essentially a superposition of two independent one dimensional diffusion systems. Further, note that, $G_1(s)$ can be obtained from $G_2(s)$ by replacing y^* and d_y in $G_2(s)$, by $(d_x - x^*)$ and d_x, respectively, and $G_2(s)$ can be obtained from $G_1(s)$ by replacing $(d_x - x^*)$ and d_x, in $G_1(s)$ by y^* and d_y, respectively. Hence, by setting

$$\breve{G}(s, a) \triangleq \frac{\cosh(a\sqrt{s})}{\sqrt{s}\sinh(\sqrt{s})}, \quad 0 \leq a \leq 1, \qquad (23)$$

we have a normalized transfer-function, from which we can not only retrieve $G_1(s)$ and $G_2(s)$,

$$G_1(s) \quad = \quad d_x \breve{G}(d_x^2 s, \frac{(d_x - x^*)}{d_x}) \tag{24}$$

and

$$G_2(s) \quad = \quad d_y \breve{G}(d_y^2 s, \frac{y^*}{d_y}), \tag{25}$$

but also the transfer-functions which arise due to different values of (x^*, y^*), by varying the parameter a.

To infer the characteristics of $\breve{G}(s,a)$, (23), first observe that the poles of $\breve{G}(s,a)$ are

$$\sigma_m \quad \triangleq \quad -m^2\pi^2, \quad m = 0, 1, 2 \ldots, \tag{26}$$

and the zeros of $\breve{G}(s,a)$ are

$$\rho_m \quad \triangleq \quad -(m - \frac{1}{2})^2 \frac{\pi^2}{a^2}, \quad m = 0, 1, 2 \ldots. \tag{27}$$

Since $\breve{G}(s,a)$ has a non-removable pole at $s = 0$, its static gain, is infinite:

$$\mid \breve{G}(0,a) \mid \quad = \quad \infty. \tag{28}$$

Using the definitions of sine and cosine hyperbolics, *i.e.*,

$$\sinh(X) \quad = \quad \frac{e^X - e^{-X}}{2} \tag{29}$$

and

$$\cosh(X) \quad = \quad \frac{e^X + e^{-X}}{2}, \tag{30}$$

in (23), we get

$$\breve{G}(s,a) \quad = \quad \frac{e^{-(1-a)\sqrt{s}}}{\sqrt{s}} \frac{1 + e^{-2a\sqrt{s}}}{1 - e^{-2\sqrt{s}}}, \quad 0 \leq a \leq 1, \tag{31}$$

which implies $\breve{G}(s,a) \to 0$ as $s \to \infty$, for all $0 \leq a \leq 1$. From (31), it is also apparent that, as a gets closer to 1, the convergence of $\breve{G}(s,a)$ to zero, as $s \to \infty$, gets slower. In fact at $a = 1$, the convergence rate drops down to $\frac{1}{\sqrt{s}}$.

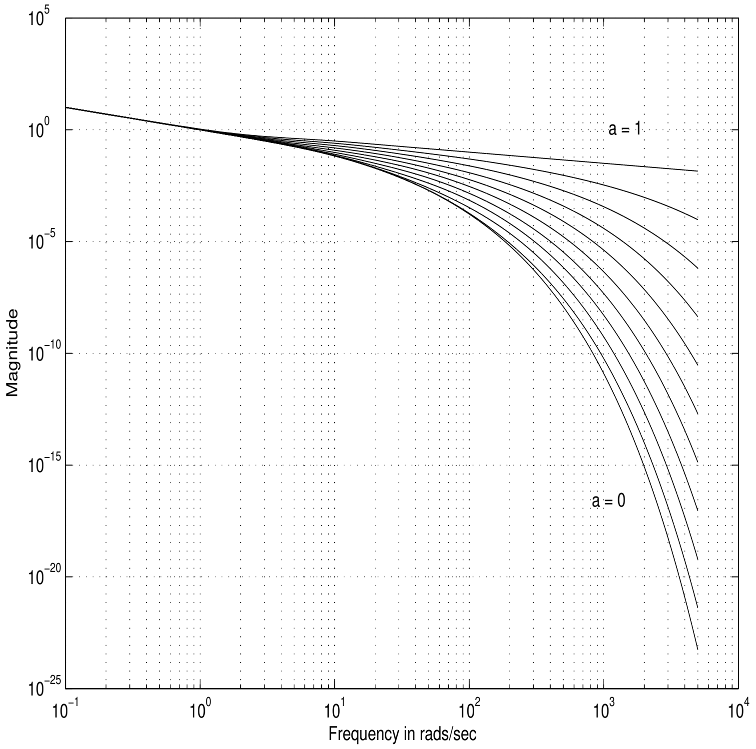

Figure 2: Plot of $| \breve{G}(i\omega, a) |$, for $a = 0.1k$, $k = 0, 1, 2 \ldots, 10$.

In Figure 2, we have plotted $\breve{G}(s,a)$, for different values of $a \in [0,1]$. As predicted, we can see that $\breve{G}(s,a) \to \infty$ as $s \to 0$, and $\breve{G}(s,a) \to 0$ as $s \to \infty$, for all a, and the rate at which $\breve{G}(s,a) \to 0$, as $s \to \infty$, decreases as a gets closer and closer to 1.

Though $\breve{G}(s,a)$, (23), characterizes the chosen LTI system (21), an alternative, but more useful, characterization of the chosen LTI system can be obtained by using operational calculus, see [7] and [14]. Using standard techniques of operational calculus, one can show that, see appendix,

$$\breve{G}(s,a) \quad = \quad \frac{1}{s-\sigma_0} + 2\sum_{l=1}^{\infty} \frac{(-1)^l \cos(l\pi a)}{s-\sigma_l}. \tag{32}$$

Since the poles, $\{\sigma_m\}_{m=1}^{\infty}$, increase as $O(m^2)$, the infinite sum (32) is summable for all s, except at the poles $s = \sigma_m$, $m = 0,1,2,\ldots$. The above characterization, though equivalent to (23), expresses the chosen LTI system as an infinite number of parallel connected first order LTI systems.

Form (24), (25) and (32) it is evident that

$$G_1(s) \quad = \quad \frac{1}{d_x}\frac{1}{s-p_0} + \frac{2}{d_x}\sum_{m=1}^{\infty} \frac{(-1)^m \cos(\frac{m\pi(d_x-x^*)}{d_x})}{s-p_m} \tag{33}$$

and

$$G_2(s) \quad = \quad \frac{1}{d_y}\frac{1}{s-q_0} + \frac{2}{d_y}\sum_{m=1}^{\infty} \frac{(-1)^m \cos(\frac{m\pi y^*}{d_y})}{s-q_m}, \tag{34}$$

where

$$p_m \quad \triangleq \quad -m^2\frac{\pi^2}{d_x^2} \quad m = 0,1,2,\ldots \tag{35}$$

and

$$q_m \quad \triangleq \quad -m^2\frac{\pi^2}{d_y^2} \quad m = 0,1,2,\ldots. \tag{36}$$

4 Notations and identities

Here, we introduce some notations and also present certain basic identities, which will be used throughout this paper.

A Kronecker product of a $k \times l$ matrix $A = (a_{ij})$ and an $m \times n$ matrix B, is an $km \times ln$ matrix

$$A \otimes B \triangleq \begin{pmatrix} a_{11}B & a_{12}B & \dots & a_{1l}B \\ a_{21}B & a_{22}B & \dots & a_{2l}B \\ \vdots & \vdots & \ddots & \vdots \\ a_{k1}B & a_{k2}B & \dots & a_{kl}B \end{pmatrix}. \tag{37}$$

The following identities holds true for the Kronecker product:
If A and B are invertible square matrices and $Z = A \otimes B$, then

$$Z^{-1} = A^{-1} \otimes B^{-1}. \tag{38}$$

It holds that

$$(A \otimes B)(C \otimes D) = AC \otimes BD, \tag{39}$$

where A, B, C and D are matrices of compatible dimensions. The proofs for (38) and (39) can be found in [17].

Let

$$e_{i,j} \triangleq \begin{pmatrix} 0 & 0 & \dots & 0 & 1 & 0 & \dots & 0 \end{pmatrix}^T, \tag{40}$$

where $j \geq i$, denote a j dimensional unit vector with a value 1 in the i^{th} position, let

$$w_{j\times 1} \triangleq \begin{pmatrix} 1 & 1 & \dots & 1 & 1 \end{pmatrix}^T_{j\times 1}, \tag{41}$$

denote a j dimensional column vector with all its elements taking a value one, and let

$$0_{j\times 1} \triangleq \begin{pmatrix} 0 & 0 & \dots & 0 & 0 \end{pmatrix}^T_{j\times 1}, \tag{42}$$

denote a j dimensional column vector with all its elements equal to zero. Finally, $I_{n\times n}$ denotes an $n \times n$ identity matrix.

5 Approximate model

In this section, we construct finite order approximations for the infinite order transfer-functions $G_1(s)$ and $G_2(s)$, (22), there exits several methods for reducing the model order of a general LTI system, see [3], [4] and [10]. Most of these methods are for the reduction of large finite order systems to smaller ones. Therefore, a direct application of these methods to the chosen problem is not possible.

Since the given LTI system, (21), arises from a PDE model, (1)-(6), a natural recipe for constructing finite order approximations for $G_1(s)$ and $G_2(s)$, would be to use PDE solvers, see [9] and [18]. Finite difference approximation, see [8], is a widely used PDE solver, which leads to approximate models that are technically reasonable to analyse.

5.1 Finite difference approximation

A finite difference (FD) approximation of a PDE is constructed by discritising the spatial domain on which the PDE is defined, by a finite set of grid points and approximating the spatial derivatives by finite-differences at the chosen grid points. For a detailed description of the FD approximation scheme see [8]. There are several ways by which one can implement the FD approximation scheme, see [2], [12] and [15] for different implementations. Our implementation here runs in similar lines to the one mentioned in [12].

Here, we discretise the spatial domain $\Omega = [0, d_x] \times [0, d_y]$ by the set of grid points,

$$(x_i, y_j) \;\; = \;\; (\frac{id_x}{m-1}, \frac{jd_y}{n-1}), \;\; i = 0, 1, \ldots, m-1, \; j = 0, 1, \ldots, n-1, \tag{43}$$

where m and n are positive integers characterizing the order of the approximation. See also Figure 3.

Let

$$T_{i,j}(t) \;\; \triangleq \;\; T(x_i, y_j, t), \tag{44}$$

denote the temperature at the node (x_i, y_j). The finite difference approximation of the PDE, (1), at the node (x_i, y_j) is given by

$$\dot{T}_{i,j}(t) = \frac{T_{i+1,j}(t) - 2T_{i,j}(t) + T_{i-1,j}(t)}{\Delta_x^2} + \frac{T_{i,j+1} - 2T_{i,j}(t) + T_{i,j-1}(t)}{\Delta_y^2}, \tag{45}$$

where

$$\Delta_x \;\; = \;\; \frac{d_x}{m-1}, \tag{46}$$

$$\Delta_y \;\; = \;\; \frac{d_y}{n-1} \tag{47}$$

and $i = 0, 1, \ldots, m-1$ and $j = 0, 1, \ldots, n-1$.

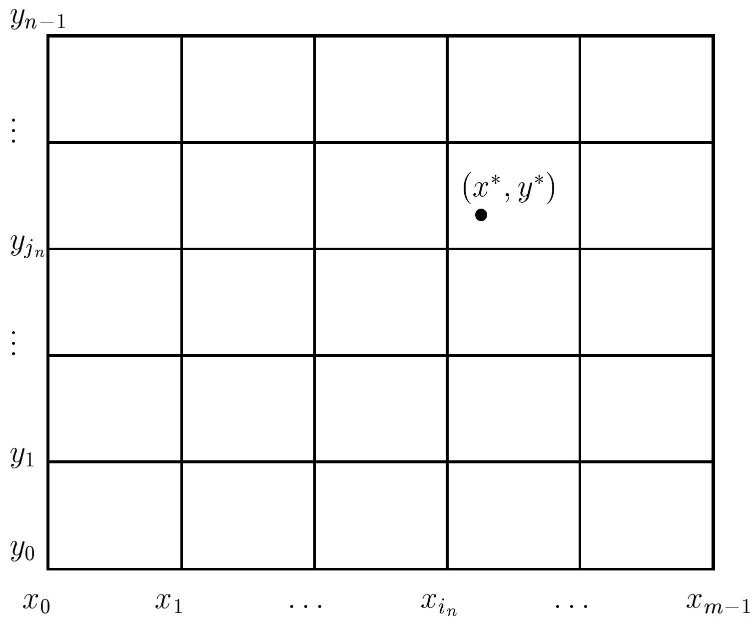

Figure 3: Discretized spatial domain Ω with (x_{i_n}, y_{j_n}) being the point closest to the desired point (x^*, y^*)

To impose the boundary condition (2) at $x = 0$, we approximate (2) by its central finite difference

$$\begin{aligned}\frac{\partial T_{0,j}(t)}{\partial x} &= \frac{T_{1,j}(t) - T_{-1,j}(t)}{2\Delta_x} \\ &= -q_1(t), \end{aligned} \tag{48}$$

which yields

$$T_{-1,j}(t) = T_{1,j}(t) + 2\Delta_x q_1(t). \tag{49}$$

Here $T_{-1,j}(t)$, $j = 0, 1, \ldots, n-1$, are dummy variables, which have no physical significance. They are introduced to impose the boundary conditions on the difference equations (45). It must be mentioned that, there are many other ways to impose the boundary conditions on a discretized PDE, see [2] and [15] for a few examples. Some of them may not involve the introduction of dummy variables. We prefer the above implementation as it leads to expressions which makes our analysis technically easier.

Similarly, at the boundaries $y = 0$, $x = d_x$ and $y = d_y$, we replace the boundary conditions (3), (4) and (5) by their respective central finite differences, and obtain, as in (48) and (49),

$$T_{i,-1}(t) = T_{i,1}(t), \tag{50}$$

$$T_{n,j}(t) = T_{n-2,j}(t) \tag{51}$$

and

$$T_{i,n}(t) = T_{i,n-2}(t) + 2\Delta_y q_2(t), \tag{52}$$

where $i = 0, 1, \ldots, m-1$ and $j = 0, 1, \ldots, n-1$.

Let $i_m < m - 1$ and $j_n < n - 1$ be two fixed positive integers, such that the grid point (x_{i_m}, y_{i_n}) is closest in distance to the desired point (x^*, y^*) in the discretized grid, see Figure 3. Hence for a large m and n, one can assume that

$$\begin{aligned} x_{i_m} &= \frac{(i_m - 1)d_x}{m-1} \\ &\approx x^* \end{aligned} \tag{53}$$

and

$$\begin{aligned} y_{i_m} &= \frac{(j_n - 1)d_y}{n-1} \\ &\approx y^*. \end{aligned} \tag{54}$$

Then the model output $T(x_{i_m}, y_{j_n}, t)$ can be taken as good approximation of the desired system output $T(x^*, y^*, t)$.

5.2 State-space representation

In this subsection, we re-write the approximate model characterized by the equations (45), (49), (50), (51) and (52) in the standard state space form.

Let

$$T_k(t) \triangleq \left[\begin{array}{ccccc} T_{k,0}(t) & T_{k,1}(t) & \ldots & T_{k,n-2}(t) & T_{k,n-1}(t) \end{array} \right]^T_{n\times 1}, \tag{55}$$

where $k = 0, 1, \ldots, m-1$, and

$$T(t) \triangleq \left[\begin{array}{ccccc} T_0^T(t) & T_1^T(t) & \ldots & T_{m-2}^T(t) & T_{m-1}^T(t) \end{array} \right]^T_{mn\times 1}. \tag{56}$$

Using (56) as the state-vector, we rewrite the equations (45), (49), (50), (51) and (52) in the standard state space form,

$$\begin{array}{rcl} \dot{T}(t) & = & AT(t) + Bq(t) \\ \\ y & = & CT(t). \end{array} \tag{57}$$

The $mn \times mn$ state-matrix A is given by

$$A \triangleq \left[\begin{array}{ccccccc} \psi_1 & \psi_3 & 0 & 0 & 0 & \ldots & 0 \\ \psi_2 & \psi_1 & \psi_2 & 0 & 0 & \ldots & 0? \\ 0 & \psi_2 & \psi_1 & \psi_2 & 0 & \ldots & 0 \\ \vdots & & & \ddots & & & \vdots \\ 0 & \ldots & 0 & \psi_2 & \psi_1 & \psi_2 & 0 \\ 0 & \ldots & 0 & 0 & \psi_2 & \psi_1 & \psi_2 \\ 0 & \ldots & 0 & 0 & 0 & \psi_3 & \psi_1 \end{array} \right]_{mn\times mn}, \tag{58}$$

$$\psi_1 \triangleq \left[\begin{array}{ccccccc} -a & 2c & 0 & 0 & 0 & \ldots & 0 \\ c & -a & c & 0 & 0 & \ldots & 0 \\ 0 & c & -a & c & 0 & \ldots & 0 \\ \vdots & & & \ddots & & & \vdots \\ 0 & \ldots & 0 & c & -a & c & 0 \\ 0 & \ldots & 0 & 0 & c & -a & c \\ 0 & \ldots & 0 & 0 & 0 & 2c & -a \end{array} \right]_{n\times n}, \tag{59}$$

$$
\begin{aligned}
\psi_2 &\triangleq bI_{n\times n}, && (60)\\
\psi_3 &\triangleq 2bI_{n\times n}, && (61)\\
a &\triangleq -2\left(\frac{1}{\Delta_x^2}+\frac{1}{\Delta_y^2}\right) && (62)\\
b &\triangleq \frac{1}{\Delta_x^2} && (63)\\
c &\triangleq \frac{1}{\Delta_y^2}. && (64)
\end{aligned}
$$

The input matrix B is given by

$$
\begin{aligned}
B &\triangleq 2\begin{bmatrix} \frac{1}{\Delta_x}w_{n\times 1} & \frac{1}{\Delta_y}e_{n,n} \\ 0 & \frac{1}{\Delta_y}e_{n,n} \\ 0 & \frac{1}{\Delta_y}e_{n,n} \\ \vdots & \vdots \\ 0 & \frac{1}{\Delta_y}e_{n,n} \end{bmatrix}_{mn\times 2} \\
&= \begin{bmatrix} \frac{2}{\Delta_x}e_{1,m}\otimes w_{n\times 1} & \frac{2}{\Delta y}w_{m\times 1}\otimes e_{n,n} \end{bmatrix} \qquad (65)
\end{aligned}
$$

where $e_{1,m}$ and $e_{n,n}$ are defined in (40), $w_{n\times 1}$ and $w_{m\times 1}$ are defined in (41). The input $q(t)$ is given by

$$q(t) \triangleq \begin{bmatrix} q_1(t) & q_2(t) \end{bmatrix}^T. \qquad (66)$$

The output matrix C is given by

$$C \triangleq e_{i_m,m}^T \otimes e_{j_n,n}^T, \qquad (67)$$

where i_m and j_n are integers as mentioned in subsection 5.1, $e_{i_m,m}$ and $e_{j_n,n}$ are as mentioned in (40). The output $y(t) \triangleq T(x_{i_m}, y_{j_n}, t)$, is the temperature at the grid point (x_{i_m}, y_{j_n}).

5.3 Transfer-function form

In the previous subsection, we characterized the approximate model in the state-space form (57). Here, we obtain the analytic expressions for the transfer-functions corresponding to (57).

In a related work, see [15], the author has constructed finite order approximations for a one dimensional heat diffusion system. The heat diffusion system considered in [15], is modeled by a PDE, which is a one dimensional version of the PDE (1), having appropriate boundary conditions. As in here, the author of [15] has constructed the approximate models using the FD approximation scheme. Not surprisingly, the results presented in this paper bear some similarity with results presented in [15]. Nevertheless, neither the problem considered in this paper nor the results presented here are trivial extensions of those in [15]. Moreover, the machinery used in [15], to obtain the results, is different from that used in this paper.

It is well known that if an LTI system is diagonalizable, then the corresponding diagonal system has the same transfer-function as the initial non-diagonal system. In system theory terminology, diagonalization of an LTI system only leads to another realization of the initially non-diagonal system. Here, we try to diagonalize the approximate system (57), in order to obtain compact and elegant expressions for its transfer-function.

Theorem 1. *The mn eigen-values of the state matrix A, (59), are*

$$\lambda_{k,l}^{m,n} \triangleq 2(b\cos(\frac{\pi k}{m-1}) + c\cos(\frac{\pi l}{n-1})) - a, \tag{68}$$

and the corresponding eigen-vectors are

$$h_{k,l} \triangleq u_k \otimes v_l, \tag{69}$$

where

$$u_k \triangleq \left[\begin{array}{ccccc} 1 & \cos(\frac{\pi k}{m-1}) & \cos(\frac{2\pi k}{m-1}) & \ldots & \cos(\pi k) \end{array}\right]^T, \tag{70}$$

and

$$v_l \triangleq \left[\begin{array}{ccccc} 1 & \cos(\frac{\pi l}{n-1}) & \cos(\frac{2\pi l}{n-1}) & \ldots & \cos(\pi l) \end{array}\right]^T, \tag{71}$$

a, b and c are as defined in (62),(63) and (64), respectively, with the indices $k = 0, 1, 2, \ldots, m-1$ and $l = 0, 1, 2, \ldots, n-1$.

Proof. See appendix.

Let

$$
\begin{aligned}
U_m &\triangleq \begin{bmatrix} u_0 & u_1 & u_2 & \dots & u_{m-1} \end{bmatrix}^T, \\
&= \begin{bmatrix}
1 & 1 & 1 & \dots & 1 \\
1 & \cos(\frac{\pi}{m-1}) & \cos(\frac{2\pi}{m-1}) & \dots & \cos(\pi) \\
1 & \cos(\frac{2\pi}{m-1}) & \cos(\frac{4\pi}{m-1}) & \dots & \cos(2\pi) \\
\vdots & \vdots & \vdots & \vdots & \vdots \\
1 & \cos(\pi) & \cos(2\pi) & \dots & \cos((m-1)\pi)
\end{bmatrix}. \qquad (72)
\end{aligned}
$$

$$
\begin{aligned}
V_n &\triangleq \begin{bmatrix} v_0 & v_1 & v_2 & \dots & v_{n-1} \end{bmatrix}^T \\
&= \begin{bmatrix}
1 & 1 & 1 & \dots & 1 \\
1 & \cos(\frac{\pi}{n-1}) & \cos(\frac{2\pi}{n-1}) & \dots & \cos(\pi) \\
1 & \cos(\frac{2\pi}{n-1}) & \cos(\frac{4\pi}{n-1}) & \dots & \cos(2\pi) \\
\vdots & \vdots & \vdots & \vdots & \vdots \\
1 & \cos(\pi) & \cos(2\pi) & \dots & \cos((n-1)\pi)
\end{bmatrix}. \qquad (73)
\end{aligned}
$$

and

$$H \triangleq U_m \otimes V_n. \qquad (74)$$

Note that by definition H, (74), is an $mn \times mn$ matrix with the eigen-vectors $h_{k,l}$, (69), of the state matrix A as its columns. Hence, if H is invertible, then A is diagonalizable. We now show that the $mn \times mn$ matrix H, (74), is invertible.

Theorem 2. *The matrices U_m and V_n, as defined in (72) and (73) respectively, are invertible and their inverses are given by*

$$
U_m^{-1} = \frac{2}{m-1}\begin{bmatrix}
\frac{1}{4} & \frac{1}{2} & \frac{1}{2} & \dots & \frac{1}{4} \\
\frac{1}{2} & \cos(\frac{\pi}{m-1}) & \cos(\frac{2\pi}{m-1}) & \dots & \frac{\cos(\pi)}{2} \\
\frac{1}{2} & \cos(\frac{2\pi}{m-1}) & \cos(\frac{4\pi}{m-1}) & \dots & \frac{\cos(2\pi)}{2} \\
\vdots & \vdots & \vdots & \vdots & \vdots \\
\frac{1}{2} & \cos(\frac{(m-2)\pi}{m-1}) & \cos(\frac{2(m-2)\pi}{m-1}) & \dots & \frac{\cos((n-2)\pi)}{2} \\
\frac{1}{4} & \frac{\cos(\pi)}{2} & \frac{\cos(2\pi)}{2} & \dots & \frac{\cos((m-1)\pi)}{4}
\end{bmatrix} \qquad (75)
$$

and

$$
V_n^{-1} = \frac{2}{n-1}\begin{bmatrix}
\frac{1}{4} & \frac{1}{2} & \frac{1}{2} & \dots & \frac{1}{4} \\
\frac{1}{2} & \cos(\frac{\pi}{n-1}) & \cos(\frac{2\pi}{n-1}) & \dots & \frac{\cos(\pi)}{2} \\
\frac{1}{2} & \cos(\frac{2\pi}{n-1}) & \cos(\frac{4\pi}{n-1}) & \dots & \frac{\cos(2\pi)}{2} \\
\vdots & \vdots & \vdots & \vdots & \vdots \\
\frac{1}{2} & \cos(\frac{(n-2)\pi}{n-1}) & \cos(\frac{2(n-2)\pi}{n-1}) & \dots & \frac{\cos((n-2)\pi)}{2} \\
\frac{1}{4} & \frac{\cos(\pi)}{2} & \frac{\cos(2\pi)}{2} & \dots & \frac{\cos((n-1)\pi)}{4}
\end{bmatrix}. \qquad (76)
$$

Proof. See appendix

Hence, using Theorem 2 and (38), we have

$$H^{-1} = U_m^{-1} \otimes V_n^{-1}. \tag{77}$$

Since H is invertible, from elementary linear algebra we know that $H^{-1}AH$ is a diagonal matrix with its diagonal elements being the eigen-values of A. More explicitly

$$H^{-1}AH = \begin{bmatrix} D_0 & & & 0 \\ & D_1 & & \\ & & \ddots & \\ 0 & & & D_{m-1} \end{bmatrix}, \tag{78}$$

where each D_k is a diagonal $n \times n$ matrix such that,

$$D_k \triangleq \begin{bmatrix} \lambda_{k,0}^{m,n} & & & 0 \\ & \lambda_{k,1}^{m,n} & & \\ & & \ddots & \\ 0 & & & \lambda_{k,n-1}^{m,n} \end{bmatrix} \tag{79}$$

and $\lambda_{k,l}^{m,n}$, $k = 0, 1, \ldots, m-1$ and $l = 0, 1, \ldots, n-1$ are as in (68).

Thus using the linear transformation

$$\bar{T}(t) = H^{-1}T(t), \tag{80}$$

on the state-vector of (57), we arrive at the desired diagonal system

$$\begin{aligned} \dot{\bar{T}}(t) &= \bar{A}\bar{T}(t) + \bar{B}u(t) \\ y(t) &= \bar{C}\bar{T}(t), \end{aligned} \tag{81}$$

where

$$\bar{A} \triangleq H^{-1}AH, \tag{82}$$

$$\bar{B} \triangleq H^{-1}B \tag{83}$$

and

$$\bar{C} \triangleq CH. \tag{84}$$

To get a complete description of the diagonal system, (81), one has to calculate the products $H^{-1}B$ and CH.

Since, see (65),

$$B \;=\; \begin{bmatrix} \frac{2}{\Delta_x} e_{1,m} \otimes w_{n\times 1} & \frac{2}{\Delta_y} w_{m\times 1} \otimes e_{n,n} \end{bmatrix}, \tag{85}$$

the first column of the product $H^{-1}B$ is given by

$$\begin{aligned} \frac{2}{\Delta_x} H^{-1}(e_{1,m} \otimes w_{n\times 1}) &= \frac{2}{\Delta_x}(U_m^{-1} \otimes V_n^{-1})(e_{1,m} \otimes w_{n\times 1}) \\ &= \frac{2}{\Delta_x}(U_m^{-1} e_{1,m}) \otimes (V_n^{-1} w_{n\times 1}). \end{aligned} \tag{86}$$

Note that, from (40) and (75),

$$U_m^{-1} e_{1,m} \;=\; \frac{2}{m-1} \begin{bmatrix} \frac{1}{4} \\ \frac{1}{2} \\ \frac{1}{2} \\ \vdots \\ \frac{1}{2} \\ \frac{1}{4} \end{bmatrix} \tag{87}$$

Similarly, from (41) and (76)

$$V_n^{-1} w_{n\times 1} \;=\; \frac{2}{n-1} \begin{bmatrix} \frac{n-1}{2} \\ \sum_{j=0}^{n-1} \frac{\cos(j\frac{\pi}{n-1})}{c_j} \\ \sum_{j=0}^{n-1} \frac{\cos(j\frac{2\pi}{n-1})}{c_j} \\ \vdots \\ \sum_{j=0}^{n-1} \frac{\cos(j\frac{(n-2)\pi}{n-1})}{c_j} \\ \frac{1}{2}\sum_{j=0}^{n-1} \frac{\cos(j\pi)}{c_j} \end{bmatrix}, \tag{88}$$

where

$$c_j = \begin{cases} 2 & j = 0 \text{ and } j = n-1 \\ 1 & j = 1, 2, \ldots, n-2. \end{cases} \tag{89}$$

It is known that, see Lemma 3, in appendix,

$$\begin{aligned}\frac{2}{(n-1)c_i}\sum_{j=0}^{n-1}\frac{\cos(j\frac{i\pi}{n-1})}{c_j} &= \delta_{i,0} \\ &= 0 \;\; \forall\, i=1,2,\ldots,n-1, \qquad (90)\end{aligned}$$

where $\delta_{j,k}$ is the Kronecker delta. Hence

$$\begin{aligned}V_n^{-1}w_{n\times 1} &= \begin{bmatrix}1\\0\\0\\\vdots\\0\end{bmatrix} \\ &= e_{1,n}. \qquad (91)\end{aligned}$$

Therefore using (43), (87) and (91) in (86), we have

$$\begin{aligned}\frac{2}{\Delta_x}H^{-1}(e_{1,m}\otimes w_{n\times 1}) &= \frac{4}{d_x}\begin{bmatrix}\frac{1}{4}e_{1,n}\\ \frac{1}{2}e_{1,n}\\ \frac{1}{2}e_{1,n}\\ \vdots \\ \frac{1}{2}e_{1,n}\\ \frac{1}{4}e_{1,n}\end{bmatrix} \\ &\triangleq \bar{B}_1. \qquad (92)\end{aligned}$$

Using the notation

$$\bar{B}_1 \triangleq \begin{bmatrix} \bar{b}^1_{0,0} \\ \bar{b}^1_{0,1} \\ \bar{b}^1_{0,2} \\ \vdots \\ \bar{b}^1_{0,n-1} \\ \bar{b}^1_{1,0} \\ \bar{b}^1_{1,1} \\ \vdots \\ \bar{b}^1_{1,n-1} \\ \vdots \\ \bar{b}^1_{m-1,0} \\ \vdots \\ \bar{b}^1_{m-1,n-1} \end{bmatrix}, \tag{93}$$

it holds that

$$\bar{b}^1_{k,l} = \begin{cases} 0 & k = 0, 1, 2, \ldots, m-1 \text{ and } l = 1, \ldots, n-1 \\ \frac{1}{d_x} & k = 0, m-1 \text{ and } l = 0 \\ \frac{2}{d_x} & k = 1, 2, \ldots, m-2 \text{ and } l = 0. \end{cases} \tag{94}$$

Next, consider the second column of $H^{-1}B$, which is

$$\frac{2}{\Delta_y}(U_m^{-1} \otimes V_n^{-1})(w_{m\times 1} \otimes e_{n,n}) \;=\; \frac{2}{\Delta_y}(U_m^{-1} w_{m\times 1}) \otimes (V_n^{-1} e_{n,n}).$$

From (91), we can see that the first product

$$U_m^{-1} w_{m\times 1} \;=\; e_{1,m}. \tag{95}$$

For the second product, $V_n^{-1}e_{n,n}$, note that, it corresponds to the last column of V_n^{-1}. Using (76),

$$V_n^{-1}e_{n,n} \quad = \quad \frac{2}{n-1}\begin{bmatrix} \frac{1}{4} \\ \frac{-1}{2} \\ \frac{1}{2} \\ \vdots \\ \frac{(-1)^{n-2}}{2} \\ \frac{(-1)^{n-1}}{4} \end{bmatrix}. \tag{96}$$

Using (43), (95) and (96) in (95), we get

$$\frac{2}{\Delta_y}(U_m^{-1} \otimes V_n^{-1})(w_{m\times 1} \otimes e_{n,n}) \quad = \quad \frac{4}{d_y}\begin{bmatrix} g \\ 0_{n\times 1} \\ 0_{n\times 1} \\ \vdots \\ 0_{n\times 1} \end{bmatrix} \tag{97}$$

$$\triangleq \quad \bar{B}_2, \tag{98}$$

where

$$g \quad \triangleq \quad \begin{bmatrix} \frac{1}{4} \\ \frac{-1}{2} \\ \frac{1}{2} \\ \vdots \\ \frac{(-1)^{n-2}}{2} \\ \frac{(-1)^{n-1}}{4} \end{bmatrix} \tag{99}$$

and $0_{n\times 1}$ is defined in (42).

With the notation

$$\bar{B}_2 \triangleq \begin{bmatrix} \bar{b}^2_{0,0} \\ \bar{b}^2_{0,1} \\ \bar{b}^2_{0,2} \\ \vdots \\ \bar{b}^2_{0,n-1} \\ \bar{b}^2_{1,0} \\ \bar{b}^2_{1,1} \\ \vdots \\ \bar{b}^2_{1,n-1} \\ \vdots \\ \bar{b}^2_{m-1,0} \\ \vdots \\ \bar{b}^2_{m-1,n-1} \end{bmatrix}. \tag{100}$$

it holds that

$$\bar{b}^2_{k,l} = \begin{cases} 0 & k = 1, 2, \ldots, m-1 \text{ and } l = 0, 1, \ldots, n-1 \\ \frac{(-1)^k}{d_y} & k = 0 \text{ and } l = 0, n-1 \\ \frac{2(-1)^k}{d_y} & k = 0 \text{ and } l = 1, 2, \ldots, n-2. \end{cases} \tag{101}$$

Finally, consider the $mn \times 1$ row-vector $\bar{C}$. Note that

$$\begin{aligned} \bar{C} &= CH \\ &= (e^T_{i_m,m} \otimes e^T_{j_n,n})(U_m \otimes V_n) \\ &= (e^T_{i_m,m} U_m) \otimes (e^T_{j_n,n} V_n). \end{aligned} \tag{102}$$

The product $e_{i_m,m}^T U_m$ in (102) is the i_m^{th} row of U_m,

$$e_{i_m,m}^T U_m \;=\; \left[\begin{array}{cccc} 1 & \cos((i_m-1)\frac{\pi}{m-1}) & \ldots & \cos((i_m-1)\pi) \end{array}\right], \qquad (103)$$

and similarly $e_{j_n,n}^T V_n$ is the j_n^{th} row of V_n,

$$w_{j_n} V_n \;=\; \left[\begin{array}{cccc} 1 & \cos((j_n-1)\frac{\pi}{n-1}) & \ldots & \cos((j_n-1)\pi) \end{array}\right]. \qquad (104)$$

Hence, if

$$\bar{C} \;\triangleq\; \left[\begin{array}{ccccccccc} \bar{c}_{0,0} & \bar{c}_{0,1} & \ldots & \bar{c}_{0,n-1} & \bar{c}_{1,0} & \ldots & \bar{c}_{1,n-1} & \ldots & \ldots & \bar{c}_{m-1,n-1} \end{array}\right], \qquad (105)$$

then

$$\bar{c}_{k,l} = \cos((i_m-1)\frac{k\pi}{m-1})\cos((j_n-1)\frac{l\pi}{n-1}), \qquad (106)$$

where $k = 0, 1, \ldots, m-1$ and $l = 0, 1, \ldots, n-1$.

Note that

$$\begin{aligned} \cos((i_m-1)\frac{k\pi}{m-1}) &= \cos(\frac{(i_m-1)d_x}{(m-1)}\frac{k\pi}{d_x}) \\ &= \cos(\frac{k\pi x_{i_m}}{d_x}) \end{aligned} \qquad (107)$$

and

$$\begin{aligned} \cos((j_n-1)\frac{l\pi}{n-1}) &= \cos(\frac{(j_n-1)d_y}{(n-1)}\frac{l\pi}{d_y}) \\ &= \cos(\frac{l\pi y_{j_n}}{d_y}). \end{aligned} \qquad (108)$$

Hence

$$\bar{c}_{k,l} = \cos(\frac{k\pi x_{i_m}}{d_x})\cos(\frac{l\pi y_{j_n}}{d_y}). \qquad (109)$$

Having characterized the diagonal system (81), we now move on to determine its transfer-function.

Note that, the transfer-function corresponding to (81) are given by

$$G_1^m(s) \;\triangleq\; \bar{C}(sI_{mn\times mn} - \bar{A})^{-1}\bar{B}_1 \qquad (110)$$

and

$$G_2^m(s) \;\triangleq\; \bar{C}(sI_{mn\times mn} - \bar{A})^{-1}\bar{B}_2, \qquad (111)$$

where $\bar{A}$, $\bar{B}_1$, $\bar{B}_2$ and $\bar{C}$ are as in (82), (94), (101) and (106) respectively. Since $\bar{A}$ is diagonal, $\bar{B}_1$ and $\bar{B}_2$ have only m and n non-zero elements, respectively, it can be checked that, see appendix,

$$G_1^m(s) = \frac{1}{d_x}\sum_{k=0}^{m-1}\frac{\alpha_k\cos(\frac{k\pi x_{i_m}}{d_x})}{s-\lambda_{k,0}^{m,n}}, \tag{112}$$

and

$$G_2^n(s) = \frac{1}{d_y}\sum_{l=0}^{n-1}\frac{(-1)^l\beta_l\cos(\frac{l\pi y_{j_n}}{d_y})}{s-\lambda_{0,l}^{m,n}}, \tag{113}$$

where

$$\alpha_k \triangleq \begin{cases} 1 & k=0 \text{ and } m-1 \\ 2 & k=1,2,\ldots,m-2 \end{cases} \tag{114}$$

and

$$\beta_l \triangleq \begin{cases} 1 & l=0 \text{ and } n-1 \\ 2 & l=1,2,\ldots,n-2. \end{cases} \tag{115}$$

Note that

$$\begin{aligned} \cos(\frac{k\pi x_{i_m}}{d_x}) &= (-1)^k(-1)^k\cos(\frac{k\pi x_{i_m}}{d_x}) \\ &= (-1)^k\cos(k\pi)\cos(\frac{k\pi x_{i_m}}{d_x}) \\ &= (-1)^k\cos(k(1-\frac{x_{i_m}}{d_x})\pi) \\ &= (-1)^k\cos(\frac{(d_x-x_{i_m})k\pi}{d_x}). \end{aligned} \tag{116}$$

Using (116) in (112), we get

$$G_1^m(s) = \frac{1}{d_x}\sum_{k=0}^{m-1}\frac{(-1)^k\alpha_k\cos(\frac{(d_x-x_{i_m})k\pi}{d_x})}{s-\lambda_{k,0}^{m,n}}. \tag{117}$$

which is similar in structure to $G_2^n(s)$, (113).

Note that $G_1^m(s)$ and $G_1^n(s)$ are rational functions of order m and n, respectively, in the standard partial fraction form. Hence, if the LTI system,

$$Y(s) = [G_1^m(s)\ ,\ G_2^n(s)]\,U(s), \tag{118}$$

is represented in the time domain, the corresponding state-space model will be of order $m+n$. The state-space model (81) is effectively of order $m+n$. This can also be infered from the fact that, the state-matrix $\bar{A}$ is diagonal, $\bar{B}_1$ has only m non-zero elements and $\bar{B}_2$ has only n non-zero elements. Hence, diagonalization has lead to a realization of model order $m+n$, as opposed to the initial non-diagonal system (57), which has a higher model order mn. Moreover, note that, the approximate transfer-functions $G_1^m(s)$, (117), and $G_1^n(s)$, (113), are similar in structure to the true transfer-functions $G_1(s)$ and $G_2(s)$, see (33) and (34). And like the true transfer-functions $G_1(s)$ and $G_2(s)$, the approximate transfer-functions $G_1^m(s)$ and $G_1^n(s)$ decouples the LTI system (118) into two independent one dimensional LTI systems.

6 Asymptotic analysis of the approximate transfer-functions

It is well known that for the chosen problem, the approximate model (57) converges to the PDE model, (1)-(6), as $\Delta_x \to 0$ and $\Delta_y \to 0$. Hence, as a consequence, the approximate transfer-functions $G_1^m(s)$, (117) and $G_2^n(s)$, (113), also converge to their respective true transfer-functions $G_1(s)$, (33), and $G_2(s)$, (34), as m and n tend to infinity. Even though the convergence of the approximate transfer-functions to the true transfer-functions is an established fact, here, we analyze the convergence, as it would throw more light on the rate of convergence.

Note, from (68), that

$$\begin{aligned}
\lambda_{k,l}^{m,n} &= 2(b\cos(\frac{\pi k}{m-1}) + c\cos(\frac{\pi l}{n-1})) - a \\
&= -\frac{2}{\Delta_x^2}\left(1-\cos(\frac{\pi k}{m-1})\right) - \frac{2}{\Delta_y^2}\left(1-\cos(\frac{\pi l}{n-1})\right) \\
&= -2\frac{(m-1)^2}{d_x^2}\left(1-\cos(\frac{\pi k}{m-1})\right) - 2\frac{(n-1)^2}{d_y^2}\left(1-\cos(\frac{\pi l}{n-1})\right) \\
&= -4\frac{(m-1)^2}{d_x^2}\sin^2(\frac{\pi k}{2(m-1)}) - 4\frac{(n-1)^2}{d_y^2}\sin^2(\frac{\pi l}{2(n-1)})) \\
&= -\frac{\pi^2}{d_x^2}k^2\left[\frac{\sin(\frac{\pi k}{2(m-1)})}{\frac{\pi k}{2(m-1)}}\right]^2 - \frac{\pi^2}{d_y^2}l^2\left[\frac{\sin(\frac{\pi l}{2(n-1)})}{\frac{\pi l}{2(n-1)}}\right]^2,
\end{aligned} \tag{119}$$

for any $k = 0,1,2,\ldots,n-1$ and $l = 0,1,2,\ldots,m-1$.

Hence, for a fixed k and l,

$$\begin{aligned}\lim_{n\to\infty}\lim_{m\to\infty}\lambda_{k,l}^{m,n} &= -\pi^2(\frac{k^2}{d_x^2}+\frac{l^2}{d_y^2}) \\ &\triangleq \lambda_{k,l}. \end{aligned} \tag{120}$$

Since for a given m, the abscissa x_{i_m} is the closest to the desired coordinate x^*, we can assume that

$$\lim_{m\to\infty} x_{i_m} = x^*. \tag{121}$$

Hence, for a fixed k

$$\lim_{m\to\infty}\alpha_k\cos(\frac{k\pi(d_x-x_{i_m})}{d_x}) = \begin{cases} 1 & \text{if } k=0 \\ 2\cos(\frac{k\pi(d_x-x^*)}{d_x}) & \text{if } k>0. \end{cases} \tag{122}$$

Similarly, one can also show that, for a fixed l

$$\lim_{n\to\infty}\beta_l\cos(\frac{\pi l y_{j_n}}{d_y}) = \begin{cases} 1 & \text{if } l=0 \\ 2\cos(\frac{l\pi y^*}{d_y}) & \text{if } l>0. \end{cases} \tag{123}$$

Since

$$\lambda_{k,0} = p_k,\ k=0,1,2,\ldots \tag{124}$$

and

$$\lambda_{0,l} = q_l,\ l=0,1,2,\ldots, \tag{125}$$

where p_k and q_l are the true system poles, as in (35) and (36), the true transfer-functions $G_1(s)$ and $G_2(s)$, see (33) and (34), can be written as

$$G_1(s) = \frac{1}{d_x}\frac{1}{s-\lambda_{0,0}}+\frac{2}{d_x}\sum_{k=1}^{\infty}\frac{(-1)^k\cos(\frac{k\pi(d_x-x^*)}{d_x})}{s-\lambda_{k,0}} \tag{126}$$

and

$$G_2(s) = \frac{1}{d_y}\frac{1}{s-\lambda_{0,0}}+\frac{2}{d_y}\sum_{l=1}^{\infty}\frac{(-1)^l\cos(\frac{l\pi y^*}{d_y})}{s-\lambda_{0,l}} \tag{127}$$

respectively.

Though it is apparent from (117), (113), (120), (122) and (123) that

$$\lim_{m\to\infty} G_1^m(s) = G_1(s) \tag{128}$$

and

$$\lim_{n\to\infty} G_2^n(s) = G_2(s) \tag{129}$$

we have given a proof of convergence in the appendix.

7 Truncated Model

From the last two sections, it is apparent that one can either choose

$$G^{mn}(s) \quad \triangleq \quad [G_1^m(s), G_2^n(s)], \tag{130}$$

where $G_1^m(s)$ and $G_2^n(s)$ are as defined in (117) and (113) respectively, or choose

$$\hat{G}^{mn}(s) \quad \triangleq \quad [\hat{G}_1^m(s), \hat{G}_2^n(s)], \tag{131}$$

where

$$\hat{G}_1^m(s) \quad \triangleq \quad \frac{1}{d_x}\frac{1}{s-p_0} + \frac{2}{d_x}\sum_{k=1}^{m-1}\frac{(-1)^k\cos(\frac{\pi k(d_x-x^*)}{d_x})}{s-p_k} \tag{132}$$

and

$$\hat{G}_2^n(s) \quad \triangleq \quad \frac{1}{d_y}\frac{1}{s-q_0} + \frac{2}{d_y}\sum_{l=1}^{n-1}\frac{(-1)^l\cos(\frac{l\pi y^*}{d_y})}{s-q_l}, \tag{133}$$

which are the truncations of the infinite series (126) and (127) respectively, as finite order approximations of the true transfer-functions $G_1(s)$ and $G_2(s)$.

The truncated model, (131), due to its precise pole positions would also give a good approximation of the true system. In the next section, we will compare the approximate transfer-functions (130) and (131) with the true transfer-function $G(s)$, (22), numerically for a particular case of the chosen heat diffusion system.

8 Numerical Experiments

In this section, we plot the true transfer-function $G(s)$, (22), along with the approximate transfer-functions $G^{mn}(s)$, (130), and $\hat{G}^{mn}(s)$, (131), for certain specific values of (x^*, y^*), d_x and d_y. These plots, though they do not constitute a proof, illustrate the performance of transfer-functions $G^{mn}(s)$ and $\hat{G}^{mn}(s)$ in approximating the true transfer-function $G(s)$.

In all the plots presented here, we let $d_x = d_y = 1$ and $(x^*, y^*) = (\frac{1}{2}, \frac{1}{2})$. The choice above mentioned values for d_x, d_y and (x^*, y^*), have no special significance, excepting that, they yield compact and simple expressions for the true and approximate transfer-functions, and minimizes the number of plots required to be presented.

Note that for the chosen values of d_x, d_y and (x^*, y^*), the true transfer-functions $G_1(s)$ and $G_2(s)$ are,

$$\begin{aligned} G_1(s) &= G_2(s) \\ &= \frac{\cosh(\frac{\sqrt{s}}{2})}{\sqrt{s}\sinh(\sqrt{s})}. \end{aligned} \tag{134}$$

Choosing $m-1$ and $n-1$ as even numbers, the desired points x_{i_m}, (53), and y_{j_n}, (54), are

$$\begin{aligned} x_{i_m} &= \frac{(m-1)d_x}{2(m-1)} \\ &= \frac{1}{2} \end{aligned} \tag{135}$$

and

$$\begin{aligned} y_{j_n} &= \frac{(n-1)d_y}{2(n-1)} \\ &= \frac{1}{2}. \end{aligned} \tag{136}$$

The approximate transfer-functions $G_1^m(s)$ and $G_2^n(s)$ for the chosen values are

$$G_1^m(s) = \sum_{k=0}^{m-1} \frac{(-1)^k \alpha_k \cos(\frac{k\pi}{2})}{s - \lambda_{k,0}^{m,n}}, \tag{137}$$

and

$$G_2^n(s) = \sum_{l=0}^{n-1} \frac{(-1)^l \beta_l \cos(\frac{l\pi}{2})}{s - \lambda_{0,l}^{m,n}}, \tag{138}$$

where α_k's and β_l's are as in (114) and (115), respectively, $\lambda_{k,l}^{m,n}$' s are as in (68) with

$$a = -2((m-1)^2 + (n-1)^2) \tag{139}$$

$$b = (m-1)^2 \tag{140}$$

and

$$c = (n-1)^2, \tag{141}$$

and the truncated approximations $\hat{G}_1^m(s)$ and $\hat{G}_2^n(s)$ are

$$\hat{G}_1^m(s) = \frac{1}{s-p_0} + 2\sum_{k=1}^{m-1} \frac{(-1)^k \cos(\frac{\pi k}{2})}{s-p_k} \tag{142}$$

and

$$\hat{G}_2^n(s) = \frac{1}{s-q_0} + 2\sum_{l=1}^{n-1} \frac{(-1)^l \cos(\frac{l\pi}{2})}{s-q_l} \tag{143}$$

respectively, where

$$p_n = -n^2\pi^2 \quad n = 0, 1, 2, \ldots \tag{144}$$

and

$$q_n = -n^2\pi^2 \quad n = 0, 1, 2, \ldots. \tag{145}$$

It is worth noting that for $m = n$,

$$G_1^m(s) = G_2^n(s) \tag{146}$$

and

$$\hat{G}_1^m(s) = \hat{G}_2^n(s). \tag{147}$$

Therefore to avoid too many plots, we plot the approximate transfer-functions $G_1^m(s)$, $G_2^n(s)$, $\hat{G}_1^m(s)$ and $\hat{G}_2^n(s)$ with m and n taking equal values.

From the Figures 4, 5 and 6, it is clear that the approximate transfer-functions also have low-pass characteristics with an infinite static gain. Note that even for a small moder order m, one gets a very good approximation in the low frequency regions. The approximation deteriorates with increasing frequency. An increase in the model order m improves the approximation in the high-frequency regions for both transfer-functions $\hat{G}^m(s)$ and $G^m(s)$, though the improvement does not seem to be substantial. It is apparent from Figures 4, 5 and 6, that the truncated transfer-function, $\hat{G}^m(s)$, tracks the true transfer-function $G_1(s)$ more closely than the FD approximate transfer-function $G^m(s)$, for a fixed value of m.

9 Conclusions

We conclude this paper with a brief summary highlighting the key contributions of this paper.

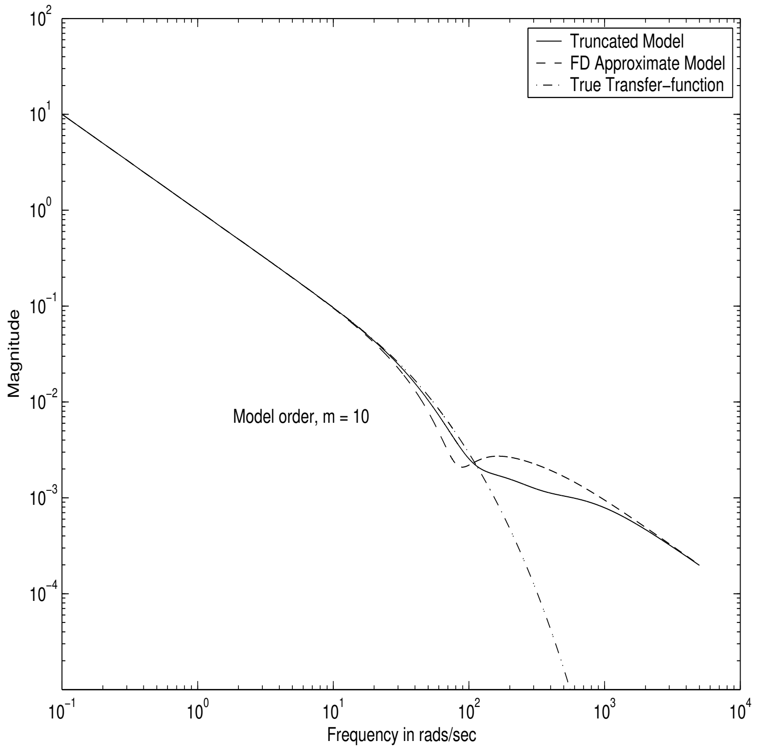

Figure 4: True transfer-function $G_1(s)$, along with the truncated transfer-function $\hat{G}_1^m(s)$ and the FD approximate transfer-function $G_1^m(s)$, for the chosen values $d_x = d_y = 1$, $(x^*, y^*) = (\frac{1}{2}, \frac{1}{2})$ and model order $m = 10$.

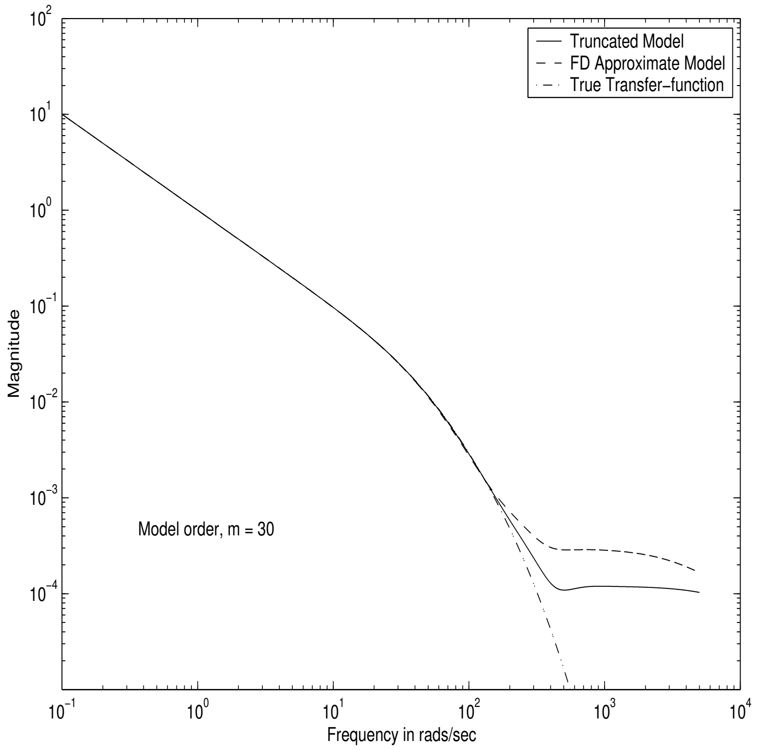

Figure 5: True transfer-function $G_1(s)$, along with the truncated transfer-function $\hat{G}_1^m(s)$ and the FD approximate transfer-function $G_1^m(s)$, for the chosen values $d_x = d_y = 1$, $(x^*, y^*) = (\frac{1}{2}, \frac{1}{2})$ and model order $m = 30$.

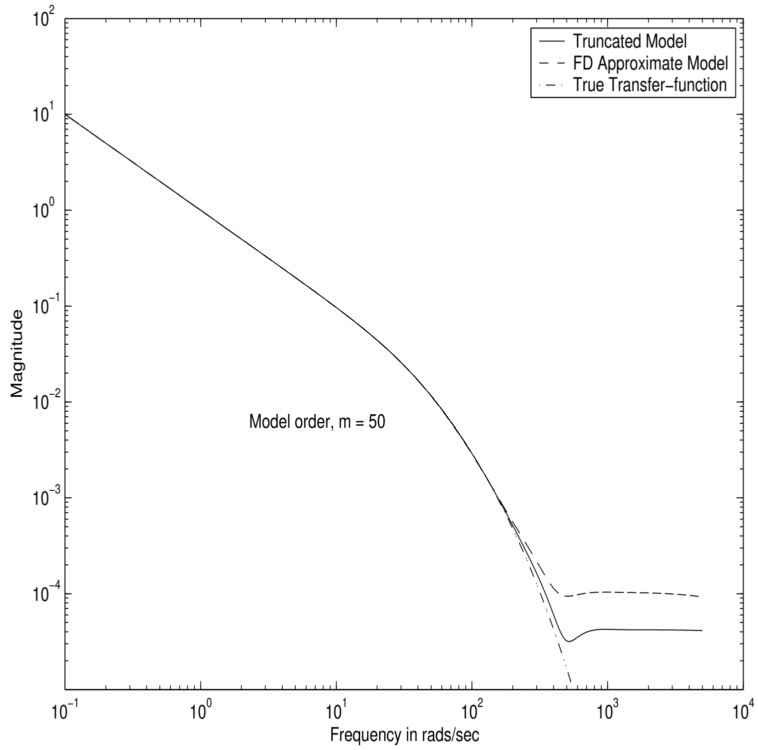

Figure 6: True transfer-function $G_1(s)$, along with the truncated transfer-function $\hat{G}_1^m(s)$ and the FD approximate transfer-function $G_1^m(s)$, for the chosen values $d_x = d_y = 1$, $(x^*, y^*) = (\frac{1}{2}, \frac{1}{2})$ and model order $m = 50$.

We have considered a two-dimensional heat diffusion system, which is modeled by a PDE, and proposed certain approximate models to compute the temperature at a desired point in the chosen system.

Our interpretation of the chosen heat diffusion system, as an LTI system with a transcendental transfer-function, and the construction of approximate models, as constructing rational approximents for the transcendental transfer-function, is different from the conventional approaches. Further, the system transfer-functions $G_1(s)$ and $G_2(s)$, (22), which characterize the chosen diffusion system, show that the system is essentially a superposition of two independent one-dimensional diffusion systems. This decoupling into two one-dimensional diffusion system is not directly evident from the PDE model, (1)-(6).

In this paper, the rational approximations, $G_1^m(s)$ and $G_2^n(s)$, were first constructed using the standard finite difference approximation scheme, and later modified by replacing their poles and zeros with respective asymptotic limits. The diagonalization procedure, which was used to get a closed form expression for the rational approximants $G_1^m(s)$ and $G_2^n(s)$, and the convergence analysis, which yielded the asymptotic poles and zeros, together provide a theoretical frame-work for analyzing and modifying the FD approximate models. This frame-work, we believe, can be applied to several other linear systems driven by a PDE, see [5], [11] and [19].

Numerical experiments performed in section 8, show that the approximate transfer-functions, $G_1^m(s)$, $G_2^n(s)$, $\hat{G}_1^m(s)$ and $\hat{G}_2^n(s)$, track their respective true transfer-functions $G_1(s)$ and $G_2(s)$, with greater accuracy in the low frequency regions than in the high frequency regions. This hence suggests that the choice of the approximation parameters m and n depends on the input spectrum. If the input spectrum has a large content of high frequency components, then m and n must be chosen adequately large to avoid any unreasonable amount of error. The above criterion provided for choosing m and n depending on the input spectrum, can also be seen as an advantage provided by frequency domain analysis of the diffusion system.

10 Appendix

10.1 Proof of the expression (32)

In this subsection, we will prove the equality (32).

Since

$$\breve{G}(s,a) = \frac{\cosh(a\sqrt{s})}{\sqrt{s}\sinh(\sqrt{s})}, \tag{148}$$

the weighting function, corresponding to the $\breve{G}(s,a)$, is given by its inverse Laplace transform

$$g(t) \triangleq \int_{\gamma-i\infty}^{\gamma+i\infty} \frac{\cosh(a\sqrt{s})}{\sqrt{s}\sinh(\sqrt{s})} e^{st} ds, \tag{149}$$

where γ is a positive real constant.

Typically integrals of the type (149) are evaluated using the Cauchy integral formula, see [14]. Since $\breve{G}(s,a) \to 0$, as $s \to \infty$, for all $0 \leq a \leq 1$, see (31), integral (149) satisfies the conditions required, see Lemma 29 and 30 in Pg 76 of [7], for a direct application of the Cauchy integral formula.

Hence, using Cauchy integral formula and evaluating (149), we get

$$\begin{aligned} g(t) &= \frac{\cosh(a\sqrt{\sigma_0})}{\frac{d}{ds}\sqrt{s}\sinh(\sqrt{s}) \mid_{s=\sigma_0}} \\ &+ \sum_{l=1}^{\infty} \frac{\cosh(a\sqrt{\sigma_l}) e^{\sigma_l t}}{\sqrt{\sigma_l}\frac{d}{ds}\sinh(\sqrt{s}) \mid_{s=\sigma_l}}, \end{aligned} \tag{150}$$

where

$$\sigma_l = -l^2\pi^2, \quad l = 0, 1, 2, \ldots, \tag{151}$$

are the poles of $\breve{G}(s,a)$.

Consider the first term of the sum (150). Since

$$\sqrt{s}\sinh(\sqrt{s}) = s + \frac{s^2}{3!} + \frac{s^3}{5!} + \ldots, \tag{152}$$

and $\sigma_0 = 0$, we have

$$\frac{d}{ds}\sqrt{s}\sinh(\sqrt{s}) \mid_{s=\sigma_0} = 1. \tag{153}$$

Therefore,

$$\frac{\cosh(a\sqrt{\sigma_0})}{\frac{d}{ds}\sqrt{s}\sinh(\sqrt{s}) \mid_{s=\sigma_0}} = 1 \tag{154}$$

Now consider an arbitrary element in the infinite sum of (150). Since,

$$\frac{d}{ds}\sinh(\sqrt{s}) = \frac{\cosh(\sqrt{s})}{2\sqrt{s}}, \tag{155}$$

we have

$$
\begin{aligned}
\frac{d}{ds}\sinh(\sqrt{s}) \mid_{s=\sigma_l} &= \frac{\cosh(\sqrt{s})}{2\sqrt{s}} \mid_{s=\sigma_l} \\
&= \frac{\cosh(il\pi)}{2\sqrt{\sigma_l}} \\
&= \frac{\cos(l\pi)}{2\sqrt{\sigma_l}} \\
&= (-1)^l \frac{1}{2\sqrt{\sigma_l}}. \qquad (156)
\end{aligned}
$$

Therefore,

$$
\begin{aligned}
\frac{\cosh(a\sqrt{\sigma_l})e^{\sigma_l t}}{\sqrt{\sigma_l}\frac{d}{ds}\sinh(\sqrt{s}) \mid_{\sigma_l}} &= \frac{\cos(al\pi)e^{\sigma_l t}}{\sqrt{\sigma_l}\frac{(-1)^l}{2\sqrt{\sigma_l}}} \\
&= 2(-1)^l\cos(al\pi)e^{\sigma_l t}. \qquad (157)
\end{aligned}
$$

Using (154) and (157) in (150), we get

$$
g(t) = 1 + 2\sum_{l=1}^{\infty}(-1)^l\cos(al\pi)e^{\sigma_l t}. \qquad (158)
$$

Laplace transformation of $g(t)$, (158), gives

$$
\begin{aligned}
\breve{G}(s,a) &= \mathcal{L}\{g(t)\} \\
&= \frac{1}{s} + 2\sum_{l=1}^{\infty}\frac{(-1)^l\cos(al\pi)}{s-\sigma_l} \\
&= \frac{1}{s-\sigma_0} + 2\sum_{l=1}^{\infty}\frac{(-1)^l\cos(al\pi)}{s-\sigma_l}, \qquad (159)
\end{aligned}
$$

which proves (32).

10.2 Proof of Theorem 1:

In this sub-section we derive the eigen-values and the eigen-vectors of the state matrix A, (58).

We first present two lemmas, which we will use to derive the eigen-values of A.

Lemma 1. *The eigen-values and the associated eigen-vectors of the matrix*

$$\psi_1 = \begin{bmatrix} -a & 2c & 0 & 0 & 0 & \dots & 0 \\ c & -a & c & 0 & 0 & \dots & 0 \\ 0 & c & -a & c & 0 & \dots & 0 \\ \vdots & & & \ddots & & & \vdots \\ 0 & \dots & 0 & c & -a & c & 0 \\ 0 & \dots & 0 & 0 & c & -a & c \\ 0 & \dots & 0 & 0 & 0 & 2c & -a \end{bmatrix}_{n\times n}, \tag{160}$$

are given by

$$\mu_k = -a + 2c\cos(\frac{k\pi}{n-1}) \tag{161}$$

and

$$v_k = \left[1 \ \cos(\frac{k\pi}{n-1}) \ \cos(\frac{2k\pi}{n-1}) \ \dots \ \cos(k\pi), \right]^T \tag{162}$$

respectively, where $k = 0, 1, 2, \dots, n-1$.

Proof. Note that solving for the eigen-value of ψ_1 is equivalent to solving for a μ such that $(\psi_1 - \mu I_{n\times n})$ is singular. Further, the null-space corresponding to μ is the eigen space of μ.

Let

$$\theta \triangleq -a - \mu \tag{163}$$

and

$$M \triangleq \begin{bmatrix} m_1 \\ M_1 \\ m_2 \end{bmatrix}_{n\times n}, \tag{164}$$

where

$$m_1 \triangleq \begin{bmatrix} \theta & 2c & 0 & \dots & 0 \end{bmatrix}_{1\times n} \tag{165}$$

$$m_2 \triangleq \begin{bmatrix} 0 & 0 & \dots & 2c & \theta \end{bmatrix}_{1\times n} \tag{166}$$

and

$$M_1 \triangleq \begin{bmatrix} c & \theta & c & & & 0 \\ & c & \theta & c & & \\ & & & \ddots & & \\ 0 & & & c & \theta & c \end{bmatrix}_{(n-2)\times n} \tag{167}$$

Let $\mathcal{N}(M)$ and $\mathcal{N}(M_1)$ denote the null spaces of the matrices M and M_1 respectively. Note that by construction $\mathcal{N}(M) \subset \mathcal{N}(M_1)$.

Here, we first characterize $\mathcal{N}(M_1)$ and determine a θ, such that $\mathcal{N}(M_1) \perp m_1$ and $\mathcal{N}(M_1) \perp m_2$.

Consider the quadratic equation

$$cz^2 + \theta z + c = 0. \tag{168}$$

Here, we assume that $c \neq 0$. Note that, if $c = 0$, then $\psi_1 = -aI_{n\times n}$, in which case the n eigen-values of ψ_1 are equal to $-a$.

Let λ be a root of the quadratic equation (168). Since $c \neq 0$, the root $\lambda \neq 0$. Note that if λ is a root of (90), then $\frac{1}{\lambda}$ is also a root of (90). Further, since

$$\theta = -c(\lambda + \frac{1}{\lambda}), \tag{169}$$

it can be checked that

$$\begin{bmatrix} c & \theta & c & & & 0 \\ & c & \theta & c & & \\ & & & \ddots & & \\ 0 & & & c & \theta & c \end{bmatrix} \begin{bmatrix} 1 & 1 \\ \lambda & \lambda^{-1} \\ \lambda^2 & \lambda^{-2} \\ \vdots & \vdots \\ \lambda^{n-1} & \lambda^{1-n} \end{bmatrix} = 0. \tag{170}$$

Note that by construction M_1 is a full rank matrix with rank $n-2$. Hence the dimension of $\mathcal{N}(M_1)$ is 2. A basis of $\mathcal{N}(M_1)$ is given by

$$\left\{ \begin{bmatrix} 1 & \lambda & \lambda^2 & \ldots & \lambda^{n-1} \end{bmatrix}^T, \begin{bmatrix} 1 & \lambda^{-1} & \lambda^{-2} & \ldots & \lambda^{1-n} \end{bmatrix}^T \right\}. \tag{171}$$

Since $\mathcal{N}(M) \subset \mathcal{N}(M_1)$, it follows that any vector $v \in \mathcal{N}(M)$ is given by

$$v = c_1 \begin{bmatrix} 1 \\ \lambda \\ \lambda^2 \\ \ldots \\ \lambda^{n-1} \end{bmatrix} + c_2 \begin{bmatrix} 1 \\ \lambda^{-1} \\ \lambda^{-2} \\ \ldots \\ \lambda^{1-n} \end{bmatrix}^T, \tag{172}$$

for some c_1 and c_2. Note that $v \perp m_1$, hence

$$v^T m_1 = 0, \tag{173}$$

which implies

$$c_1(\theta + 2c\lambda) + c_2(\theta + 2c\lambda^{-1}) = 0. \tag{174}$$

Using (169) in (174) we get

$$c_1(\lambda - \lambda^{-1}) - c_2(\lambda - \lambda^{-1}) = 0, \tag{175}$$

implying

$$c_1 = c_2. \tag{176}$$

Therefore, the null space of $\mathcal{N}(M)$, which is the eigen space of μ, is spanned by

$$v = c_1 \left[\begin{array}{ccccc} 2 & \lambda + \lambda^{-1} & \lambda^2 + \lambda^{-2} & \ldots & \lambda^{n-1} + \lambda^{1-n} \end{array} \right]^T. \tag{177}$$

Imposing the second constraint $v \perp m_2$, *i.e.*,

$$v^T m_2 = 0, \tag{178}$$

where v is as in (177), we have

$$2c(\lambda^{n-2} + \lambda^{2-n}) + \theta(\lambda^{n-1} + \lambda^{1-n}) = 0. \tag{179}$$

As before, using (169) in (179), we get

$$2c(\lambda^{n-2} + \lambda^{2-n}) - c(\lambda + \lambda^{-1})(\lambda^{n-1} + \lambda^{1-n}) = 0. \tag{180}$$

After simplification this gives

$$\lambda^n - \lambda^{n-2} - \lambda^{2-n} + \lambda^{-n} = 0. \tag{181}$$

Note that

$$\lambda^n - \lambda^{n-2} - \lambda^{2-n} + \lambda^{-n} = \lambda^{-n}(\lambda^{2(n-1)} - 1)(\lambda^2 - 1). \tag{182}$$

Hence, from (181), $\lambda = +1, -1$ or

$$\lambda = \exp(i\frac{k\pi}{n-1}) \quad k = 0, 1, 2, \ldots, 2n-3. \tag{183}$$

From (169), we can see that

$$\begin{aligned} \theta &= -c(\lambda + \lambda^{-1}) \\ &= -2c\cos(\frac{k\pi}{n-1}) \quad k = 0, 1, 2, \ldots, n-1. \end{aligned} \tag{184}$$

Since

$$\theta = -a - \mu, \tag{185}$$

see (163), the n eigen-values of ψ_1 are

$$\mu_k = -a + 2c\cos(\frac{k\pi}{n-1}) \;\; k = 0, 1, 2, \ldots, n-1. \tag{186}$$

The corresponding eigen-vectors are, see (177),

$$v_k \;\; = \;\; \begin{bmatrix} 1 \; \cos(\frac{k\pi}{n-1}) \; \cos(\frac{2k\pi}{n-1}) \; \ldots \; \cos(k\pi) \end{bmatrix}^T \tag{187}$$

where $k = 0, 1, 2, \ldots, n-1$. ■

Lemma 2. *Let*

$$\psi_1 v = \mu v \tag{188}$$

and

$$\Psi \;\; \triangleq \;\; \begin{bmatrix} \mu & 2b & & & & 0 \\ b & \mu & b & & & \\ & b & \mu & b & & \\ & & & \ddots & & \\ & & & b & \mu & b \\ 0 & & & & 2b & \mu \end{bmatrix} \tag{189}$$

be an $m \times m$ matrix. Let η and

$$u \;\; \triangleq \;\; \begin{bmatrix} u_1 \\ u_2 \\ u_3 \\ \vdots \\ u_m \end{bmatrix} \tag{190}$$

be an eigen-value eigen-vector pair of the matrix Ψ, i.e.,

$$\Psi u = \eta u. \tag{191}$$

It holds that

$$A(u \otimes v) = \eta(u \otimes v), \tag{192}$$

where

$$A = \begin{bmatrix} \psi_1 & \psi_3 & 0 & 0 & 0 & \dots & 0 \\ \psi_2 & \psi_1 & \psi_2 & 0 & 0 & \dots & 0? \\ 0 & \psi_2 & \psi_1 & \psi_2 & 0 & \dots & 0 \\ \vdots & & & \ddots & & & \vdots \\ 0 & \dots & 0 & \psi_2 & \psi_1 & \psi_2 & 0 \\ 0 & \dots & 0 & 0 & \psi_2 & \psi_1 & \psi_2 \\ 0 & \dots & 0 & 0 & 0 & \psi_3 & \psi_1 \end{bmatrix}_{mn\times mn}, \tag{193}$$

ψ_1 is as in (160)

$$\psi_2 = bI_{n\times n}, \tag{194}$$
$$\psi_3 = 2bI_{n\times n}, \tag{195}$$

and $\otimes$ denotes the Kronecker product.

Proof. Observe that, from (192),

$$\begin{bmatrix} \mu u_1 + 2bu_2 \\ bu_1 + \mu u_2 + bu_3 \\ bu_2 + \mu u_3 + bu_4 \\ \vdots \\ bu_{m-2} + \mu u_{m-1} + bu_m \\ 2bu_{m-1} + u_m \end{bmatrix} = \eta \begin{bmatrix} u_1 \\ u_2 \\ u_3 \\ \vdots \\ u_m \end{bmatrix}, \tag{196}$$

and by definition

$$u \otimes v = \begin{bmatrix} u_1 v \\ u_2 v \\ u_3 v \\ \vdots \\ u_m v \end{bmatrix}. \tag{197}$$

Hence,

$$
\begin{aligned}
A(u\otimes v) &= \begin{bmatrix} \psi_1 & 2bI & 0 & 0 & 0 & \dots & 0 \\ bI & \psi_1 & bI & 0 & 0 & \dots & 0 \\ 0 & bI & \psi_1 & bI & 0 & \dots & 0 \\ \vdots & & & \ddots & & & \vdots \\ 0 & \dots & 0 & bI & \psi_1 & bI & 0 \\ 0 & \dots & 0 & 0 & bI & \psi_1 & bI \\ 0 & \dots & 0 & 0 & 0 & 2bI & \psi_1 \end{bmatrix} \begin{bmatrix} u_1 v \\ u_2 v \\ u_3 v \\ \vdots \\ u_m v \end{bmatrix}, \\
&= \begin{bmatrix} u_1\psi_1 v + 2bu_2 v \\ bu_1 v + u_2\psi_1 v + bu_3 v \\ bu_2 v + u_3\psi_1 v + bu_4 v \\ \vdots \\ bu_{m-2}v + u_{m-1}\psi_1 v + bu_m v \\ 2bu_{m-1}v + u_m\psi_1 v \end{bmatrix}. \qquad (198)
\end{aligned}
$$

Since $\psi_1 v = \mu v$, by (188), from (198) we have

$$
\begin{aligned}
A(u\otimes v) &= \begin{bmatrix} u_1\mu v + 2bu_2 v \\ bu_1 v + u_2\mu v + bu_3 v \\ bu_2 v + u_3\mu v + bu_4 v \\ \vdots \\ bu_{m-2}v + u_{m-1}\mu v + bu_m v \\ 2bu_{m-1}v + u_m\mu v \end{bmatrix} \\
&= \begin{bmatrix} (\mu u_1 + 2bu_2)v \\ (bu_1 + \mu u_2 + bu_3)v \\ (bu_2 v + \mu u_3 + bu_4)v \\ \vdots \\ (bu_{m-2}v + \mu u_{m-1} + bu_m)v \\ (2bu_{m-1} + \mu u_m)v \end{bmatrix} \\
&= \eta \begin{bmatrix} u_1 v \\ u_2 v \\ u_3 v \\ \vdots \\ u_{m-1} v \\ u_m v \end{bmatrix} \\
&= \eta(u\otimes v). \qquad (199)
\end{aligned}
$$

The last two steps in (199) are obtained by using (196) and (197). Note that with derivation of (199) the proof of Lemma 2 is complete . ■

We now derive the eigen-values and eigen-vectors of the state-matrix A.

Since the $m \times m$ matrix Ψ, (189), has the same structure as ψ_1, (160), in Lemma 1, the eigen-value eigen-vector pair, corresponding to each μ_l, is

$$\eta_{k,l} = \mu_l + 2b\cos(\frac{k\pi}{m-1}) \tag{200}$$

$$u_k \triangleq \left[\begin{array}{ccccc} 1 & \cos(\frac{k\pi}{m-1}) & \cos(\frac{2k\pi}{m-1}) & \dots & \cos(k\pi) \end{array} \right]^T, \tag{201}$$

where $k = 0, 1, 2, \dots, m-1$. Thus, from Lemma 2, the mn eigen-values of the state matrix A are

$$\eta_{k,l} = 2(b\cos(\frac{k\pi}{m-1}) + c\cos(\frac{l\pi}{n-1})) - a, \tag{202}$$

and the corresponding eigen-vectors are

$$h_{k,l} \triangleq u_k \otimes v_l \tag{203}$$

where $k = 0, 1, 2, \dots, m-1$ and $l = 0, 1, 2, \dots, n-1$. Which finishes the proof of Theorem 1. ■

10.3 Proof of Theorem 2

In this subsection, we present a proof for Theorem 2. We base this proof on the following lemma

Lemma 3. *Let*

$$\bar{u}_k \triangleq \frac{1}{m-1} \sum_{l=0}^{m-1} \frac{\cos(\frac{lk\pi}{m-1})}{c_l}, \tag{204}$$

where m is a positive integer, $k = 0, 1, \dots, m-1$, and

$$c_j = \begin{cases} 2 & j = 0 \text{ and } j = m-1 \\ 1 & j = 1, 2, \dots, m-2. \end{cases} \tag{205}$$

It holds that

$$\bar{u}_k = \begin{cases} 1 & k = 0 \\ 0 & k = 1, 2, \dots m-1. \end{cases} \tag{206}$$

Proof. To prove (206), we compute $\bar{u}_k$, (204), for the three possible cases $k = 0$, k odd, and k even:

For $k = 0$, it is straightforward to see that $\bar{u}_0 = 1$.

Next, assume that k odd. Note that, in general

$$c_l \;=\; c_{m-1-l}, \quad l = 0, 1, \ldots, m-1, \tag{207}$$

and for k odd,

$$\cos(\frac{lk\pi}{m-1}) \;=\; -\cos(\frac{(m-1-l)k\pi}{m-1}), \quad l = 0, 1, \ldots, m-1. \tag{208}$$

Hence, using (207) and (208) in (204), we get $\bar{u}_k = 0$.

Finally, consider the case k even. Note that

$$\sum_{l=0}^{m-2} \cos(\frac{lk\pi}{m-1}) = Re\left\{\sum_{l=0}^{m-2} \exp(i\frac{lk\pi}{m-1})\right\}, \tag{209}$$

where Re denotes the real part of a complex number.

Since

$$\begin{aligned}\sum_{l=0}^{m-2} \exp(i\frac{lk\pi}{m-1}) &= \frac{1-\exp(ik\pi)}{1-\exp(i\frac{k\pi}{m-1})} \\ &= 0,\end{aligned} \tag{210}$$

we can see that

$$\begin{aligned}\sum_{l=0}^{m-1} \frac{\cos(\frac{lk\pi}{m-1})}{c_l} &= -\frac{1}{2} + \frac{(-1)^k}{2} + Re\left\{\sum_{l=0}^{m-2} \exp(i\frac{lk\pi}{m-1})\right\} \\ &= 0.\end{aligned} \tag{211}$$

Hence Lemma 3 is proved. ■

To prove that the matrix

$$U_m \;=\; \begin{bmatrix} 1 & 1 & 1 & \ldots & 1 \\ 1 & \cos(\frac{\pi}{m-1}) & \cos(\frac{2\pi}{m-1}) & \ldots & \cos(\pi) \\ 1 & \cos(\frac{2\pi}{m-1}) & \cos(\frac{4\pi}{m-1}) & \ldots & \cos(2\pi) \\ \vdots & \vdots & \vdots & \vdots & \vdots \\ 1 & \cos(\pi) & \cos(2\pi) & \ldots & \cos((m-1)\pi) \end{bmatrix} \tag{212}$$

is invertible and its inverse is

$$U_m^{-1} = \frac{2}{m-1}\begin{bmatrix} \frac{1}{4} & \frac{1}{2} & \frac{1}{2} & \dots & \frac{1}{4} \\ \frac{1}{2} & \cos(\frac{\pi}{m-1}) & \cos(\frac{2\pi}{m-1}) & \dots & \frac{\cos(\pi)}{2} \\ \frac{1}{2} & \cos(\frac{2\pi}{m-1}) & \cos(\frac{4\pi}{m-1}) & \dots & \frac{\cos(2\pi)}{2} \\ \vdots & \vdots & \vdots & \vdots & \vdots \\ \frac{1}{2} & \cos(\frac{(m-2)\pi}{m-1}) & \cos((m-2)\frac{2\pi}{m-1}) & \dots & \frac{\cos((m-2)\pi)}{2} \\ \frac{1}{4} & \frac{\cos(\pi)}{2} & \frac{\cos(2\pi)}{2} & \dots & \frac{\cos((m-1)\pi)}{4} \end{bmatrix}, \quad (213)$$

it suffices to show that $U_m \times U_m^{-1} = I_{m\times m}$.

Consider a typical element,

$$u_{r,s} \triangleq \frac{2}{m-1}\begin{bmatrix} 1 & \cos(\frac{r\pi}{m-1}) & \dots & \cos(r\pi) \end{bmatrix}\begin{bmatrix} \frac{1}{2} \\ \cos(\frac{s\pi}{m-1}) \\ \cos(\frac{2s\pi}{m-1}) \\ \vdots \\ \frac{\cos(s\pi)}{2} \end{bmatrix}, \quad (214)$$

of the product $U_m \times U_m^{-1}$, where $r = 0, 1, \dots, m-1$ and $s = 1, 2, \dots, m-2$.

Note that

$$u_{r,s} = \frac{2}{m-1}\sum_{l=0}^{m-1}\frac{\cos(\frac{lr\pi}{m-1})\cos(\frac{ls\pi}{m-1})}{c_l} \quad (215)$$

where $c_0 = c_{m-1} = 2$ and $c_l = 1, \quad l = 1, 2, \dots, m-2$.

From elementary trigonometry, we know that

$$2\cos(\frac{lr\pi}{m-1})\cos(\frac{ls\pi}{m-1}) = \cos(\frac{l(r+s)\pi}{m-1}) + \cos(\frac{l(r-s)\pi}{m-1}). \quad (216)$$

Hence

$$u_{r,s} = \frac{1}{m-1}\sum_{l=0}^{m-1}\frac{\cos(\frac{l(r+s)\pi}{m-1})}{c_l} + \frac{1}{m-1}\sum_{l=0}^{m-1}\frac{\cos(\frac{l(r-s)\pi}{m-1})}{c_l}. \quad (217)$$

From Lemma 3 we can conclude that

$$u_{r,s} = \delta_{r,s}, \quad (218)$$

where $r = 0, 1, 2, \dots, m-1$ and $s = 1, 2, \dots, m-2$.

In the case where $s = 0$, note that

$$
\begin{aligned}
u_{r,0} &= \frac{2}{m-1} \begin{bmatrix} 1 & \cos(\frac{r\pi}{m-1}) & \cos(\frac{2r\pi}{m-1}) & \ldots & \cos(r\pi) \end{bmatrix} \begin{bmatrix} \frac{1}{4} \\ \frac{1}{2} \\ \vdots \\ \frac{1}{2} \\ \frac{1}{4} \end{bmatrix} \\
&= \frac{1}{m-1} \sum_{l=0}^{m-1} \frac{\cos(\frac{lr\pi}{m-1})}{c_l}, \qquad (219)
\end{aligned}
$$

which is equal to one, if $r = 0$, and equal to zero, if $r = 1, 2, \ldots, m-1$.

Finally, for $s = m-1$, note that

$$
\begin{aligned}
u_{r,m-1} &= \frac{2}{m-1} \begin{bmatrix} 1 & \cos(\frac{r\pi}{m-1}) & \cos(\frac{2r\pi}{m-1}) & \ldots & \cos(r\pi) \end{bmatrix} \begin{bmatrix} \frac{1}{4} \\ \frac{\cos(\pi)}{2} \\ \frac{\cos(2\pi)}{2} \\ \vdots \\ \frac{\cos((m-1)\pi)}{4} \end{bmatrix} \\
&= \frac{1}{m-1} \sum_{l=0}^{m-1} \frac{\cos(\frac{lr\pi}{m-1}) \cos(l\pi)}{c_l}, \\
&= \frac{1}{m-1} \sum_{l=0}^{m-1} \frac{\cos(\frac{l(m-1+r)\pi}{m-1})}{c_l} + \frac{1}{m-1} \sum_{l=0}^{m-1} \frac{\cos(\frac{l(m-1-r)\pi}{m-1})}{c_l}. \qquad (220)
\end{aligned}
$$

which, from Lemma 3, is equal to one, if $r = m-1$ and equal to zero if $r = 0, 1, 2, \ldots, m-2$.

Therefore, from (218), (219) and (220), we have

$$u_{r,s} = \delta_{r,s} \qquad (221)$$

for $r = 0, 1, \ldots, m-1$ and $s = 0, 1, \ldots, m-1$. Hence $U_m \times U_m^{-1} = I_{m \times m}$. Similarly, it can be proved that the inverse of V_n, (73), is given by (76). ■

10.4 Proof of the expressions (112) and (113)

Here, we derive the expression (112) from (110). The derivation of (113) from (111), can be obtained in a similar fashion.

Using the definition of $\bar{A}$, see (82) and (78), we get

$$(sI_{mn\times mn} - \bar{A})^{-1} = \begin{bmatrix} D_0^n(s) & & & 0 \\ & D_1^n(s) & & \\ & & \ddots & \\ 0 & & & D_{m-1}^n(s) \end{bmatrix}, \tag{222}$$

where

$$D_k^n(s) \triangleq (sI_{n\times n} - D_k)^{-1}, \tag{223}$$

and D_k, $k = 0, 1, 2, \ldots, m-1$, are as in (79).

Since

$$D_k = \begin{bmatrix} \lambda_{k,0}^{m,n} & & & 0 \\ & \lambda_{k,1}^{m,n} & & \\ & & \ddots & \\ 0 & & & \lambda_{k,n-1}^{m,n} \end{bmatrix}, \tag{224}$$

we get

$$D_k^n(s) = \begin{bmatrix} \frac{1}{s-\lambda_{k,0}^{m,n}} & & & 0 \\ & \frac{1}{s-\lambda_{k,1}^{m,n}} & & \\ & & \ddots & \\ 0 & & & \frac{1}{s-\lambda_{k,n-1}^{m,n}} \end{bmatrix}, \tag{225}$$

Further, using (93) and (94), we can see that

$$(sI_{mn\times mn} - \bar{A})^{-1}\bar{B}_1 = \begin{bmatrix} D_0^n(s)\bar{B}_{1,0} & D_1^n(s)\bar{B}_{1,1} & \ldots & D_{m-1}^n(s)\bar{B}_{1,m-1} \end{bmatrix} \tag{226}$$

where

$$\bar{B}_{1,k} \triangleq \begin{bmatrix} \bar{b}_{k,0}^1 & \bar{b}_{k,1}^1 & \ldots & \bar{b}_{k,n-1}^1 \end{bmatrix}^T, \tag{227}$$

for $k = 0, 1, 2, \ldots, m-1$, and

$$\bar{b}_{k,l}^1 = \begin{cases} 0 & k = 0, 1, 2, \ldots, m-1 \text{ and } l = 1, \ldots, n-1 \\ \frac{1}{d_x} & k = 0, m-1 \text{ and } l = 0 \\ \frac{2}{d_x} & k = 1, 2, \ldots, m-2 \text{ and } l = 0. \end{cases} \tag{228}$$

From (227) and (228), we can infer that

$$\bar{B}_{1,0} = \left[\begin{array}{cccc} \frac{1}{d_x} & 0 & \dots & 0 \end{array} \right]^T, \tag{229}$$

$$\bar{B}_{1,l} = \frac{2}{d_x} e_{1,n}, \quad l = 1, 2, \dots m-2 \tag{230}$$

and

$$\bar{B}_{1,m-1} = \left[\begin{array}{cccc} \frac{1}{d_x} & 0 & \dots & 0 \end{array} \right]^T. \tag{231}$$

Since,

$$\bar{C} = \left[\begin{array}{ccccccccccc} \bar{c}_{0,0} & \bar{c}_{0,1} & \dots & \bar{c}_{0,n-1} & \bar{c}_{1,0} & \dots & \bar{c}_{1,n-1} & \dots & \dots & \bar{c}_{m-1,n-1} \end{array} \right], \tag{232}$$

where

$$\bar{c}_{k,l} = \cos\left(\frac{k\pi x_{i_m}}{d_x}\right) \cos\left(\frac{l\pi y_{j_n}}{d_y}\right). \tag{233}$$

see (105) and (109), we get

$$\begin{aligned} \bar{C}(sI_{mn\times mn} - \bar{A})^{-1}\bar{B}_1 &= \frac{1}{d_x} \frac{\bar{c}_{0,0}}{s - \lambda_{0,0}^{m,n}} + \frac{2}{d_x} \sum_{k=1}^{m-2} \frac{\bar{c}_{k,0}}{s - \lambda_{k,0}^{m,n}} \\ &+ \frac{1}{d_x} \frac{\bar{c}_{m-1,0}}{s - \lambda_{m-1,0}^{m,n}}. \end{aligned} \tag{234}$$

Hence

$$\bar{C}(sI_{mn\times mn} - \bar{A})^{-1}\bar{B}_1 = \frac{1}{d_x} \sum_{k=0}^{m-1} \frac{\alpha_k \cos\left(\frac{k\pi x_{i_m}}{d_x}\right)}{s - \lambda_{k,0}^{m,n}}, \tag{235}$$

where

$$\alpha_k \triangleq \begin{cases} 1 & k = 0 \text{ and } m-1 \\ 2 & k = 1, 2, \dots, m-2 \end{cases} \tag{236}$$

Hence proved. ■

10.5 Proof of convergence for (128) and (129)

Here, we present the proof of convergence for, (128),

$$\lim_{m\to\infty} G_1^m(s) = G_1(s), \tag{237}$$

where

$$\begin{aligned} G_1(s) &= \frac{1}{d_x}\frac{1}{s} + \frac{2}{d_x}\sum_{k=1}^{\infty}\frac{(-1)^k\cos(\frac{k\pi(d_x-x^*)}{d_x})}{s-\lambda_{k,0}} \\ &\triangleq \frac{1}{d_x}\frac{1}{s} + \bar{G}_1(s) \end{aligned} \tag{238}$$

and

$$\begin{aligned} G_1^m(s) &= \frac{1}{d_x}\frac{1}{s} + \frac{1}{d_x}\sum_{k=1}^{m-1}\frac{(-1)^k\alpha_k\cos(\frac{(d_x-x_{i_m})k\pi}{d_x})}{s-\lambda_{k,0}^{m,n}}, \\ &\triangleq \frac{1}{d_x}\frac{1}{s} + \bar{G}_1^m(s). \end{aligned} \tag{239}$$

Proof of convergence for (129) can be obtained in a similar fashion.

We base our proof of (237), on the following lemma.

Lemma 4. *Let $\{x_{k,m}\}_{k,m=0}^{\infty}$ and $\{c_{k,m}\}_{k,m=0}^{\infty}$ be two bounded double sequences such that, for each fixed k*

$$\lim_{m\to\infty} x_{k,m} \triangleq \bar{x}_k \quad k = 1, 2, \ldots \tag{240}$$

and

$$\lim_{m\to\infty} c_{k,m} \triangleq \bar{c}_k \quad k = 1, 2, \ldots, \tag{241}$$

where $\{\bar{x}_k\}_{k=0}^{\infty}$ and $\{\bar{c}_k\}_{k=0}^{\infty}$ are bounded sequences, with $\{\bar{c}_k\}_{k=0}^{\infty}$ being strictly positive. Further, assume that the convergence rates of (20) and (21) are such that

$$\mid x_{k,m} - \bar{x}_k \mid \;\sim\; \frac{1}{m^{\alpha_1}} \tag{242}$$

and

$$\mid c_{k,m} - \bar{c}_k \mid \;\sim\; \frac{1}{m^{\alpha_2}}, \tag{243}$$

where $\alpha_1 > 0$ and $\alpha_2 > 0$, for all $k = 1, 2, 3, \ldots$.

Let

$$y_{k,m} \triangleq b - c_{k,m}k^2 \quad k = 1, 2, \ldots \tag{244}$$

and

$$\bar{y}_k \triangleq b - \bar{c}_k k^2 \quad k = 1, 2, \ldots, \tag{245}$$

where b *is a constant, such that* $b \neq c_{k,m}k^2$ *and* $b \neq \bar{c}_k k^2$ *for all* $k = 1, 2, \ldots$ *and* $m = 1, 2, \ldots$.

Then

1.

$$\lim_{m \to \infty} \frac{x_{k,m}}{y_{k,m}} = \frac{\bar{x}_k}{\bar{y}_k}, \quad k = 1, 2, \ldots \tag{246}$$

2.

$$\mid \frac{x_{k,m}}{y_{k,m}} - \frac{\bar{x}_k}{\bar{y}_k} \mid \sim \frac{1}{k^2 m^{\alpha_{\min}}}, \tag{247}$$

where $\alpha_{\min} = \min\{\alpha_1, \alpha_2\}$, $k = 1, 2, \ldots,$ *and* $m = 1, 2, \ldots$.

and

3. *The partial sum*

$$s_m \triangleq \sum_{k=1}^{m} \mid \frac{x_{k,m}}{y_{k,m}} - \frac{\bar{x}_k}{\bar{y}_k} \mid, \tag{248}$$

converges to zero, as $m \to \infty$.

Proof. Note that

$$\begin{aligned}
\frac{x_{k,m}}{y_{k,m}} - \frac{\bar{x}_k}{\bar{y}_k} &= \frac{x_{k,m} + \bar{x}_k - \bar{x}_k}{y_{k,m} + \bar{y}_k - \bar{y}_k} - \frac{\bar{x}_k}{\bar{y}_k} \\
&= \frac{\bar{x}_k}{\bar{y}_k} \left\{ \frac{1 + \frac{x_{k,m} - \bar{x}_k}{\bar{x}_k}}{1 + \frac{y_{k,m} - \bar{y}_k}{\bar{y}_k}} - 1 \right\} \\
&= \frac{\bar{x}_k}{\bar{y}_k} \left\{ \left(1 + \frac{x_{k,m} - \bar{x}_k}{\bar{x}_k}\right) \left(1 + \frac{y_{k,m} - \bar{y}_k}{\bar{y}_k}\right)^{-1} - 1 \right\} \\
&= \frac{\bar{x}_k}{k^2(\frac{b}{k^2} - \bar{c}_k)} \left(1 + \frac{x_{k,m} - \bar{x}_k}{\bar{x}_k}\right) \left(1 - \frac{c_{k,m} - \bar{c}_k}{\frac{b}{k^2} - \bar{c}_k}\right)^{-1} \\
&- \frac{\bar{x}_k}{k^2(\frac{b}{k^2} - \bar{c}_k)}.
\end{aligned} \tag{249}$$

Since $\lim_{m\to\infty} c_{k,m} = \bar{c}_k$ for all k, for a large m we have

$$\left(1 - \frac{c_{k,m} - \bar{c}_k}{\frac{b}{k^2} - \bar{c}_k}\right)^{-1} \approx \left(1 + \frac{c_{k,m} - \bar{c}_k}{\frac{b}{k^2} - \bar{c}_k}\right). \tag{250}$$

Using (250) in (249), we have

$$\begin{aligned} \frac{x_{k,m}}{y_{k,m}} - \frac{\bar{x}_k}{\bar{y}_k} &\approx \frac{1}{k^2(\frac{b}{k^2} - \bar{c}_k)} \left\{ (x_{k,m} - \bar{x}_k) + \bar{x}_k \left(\frac{c_{k,m} - \bar{c}_k}{\frac{b}{k^2} - \bar{c}_k}\right) \right. \\ &\quad \left. + (x_{k,m} - \bar{x}_k)\left(\frac{c_{k,m} - \bar{c}_k}{\frac{b}{k^2} - \bar{c}_k}\right) \right\}, \end{aligned} \tag{251}$$

which implies

$$\begin{aligned} \mid \frac{x_{k,m}}{y_{k,m}} - \frac{\bar{x}_k}{\bar{y}_k} \mid &\leq \mid \frac{1}{k^2(\frac{b}{k^2} - \bar{c}_k)} \mid \{\mid x_{k,m} - \bar{x}_k \mid \\ &\quad + \mid \bar{x}_k \left(\frac{c_{k,m} - \bar{c}_k}{\frac{b}{k^2} - \bar{c}_k}\right) \mid \\ &\quad + \mid (x_{k,m} - \bar{x}_k)\left(\frac{c_{k,m} - \bar{c}_k}{\frac{b}{k^2} - \bar{c}_k}\right) \mid \Bigg\}. \end{aligned} \tag{252}$$

Since $\bar{x}_k$ and $\frac{b}{k^2} - \bar{c}_k$ are non-zero and bounded for all k, from (242), (243) and (252) it is clear that both (246) and (247) holds true.

From (247), it can be infered that there exits a constant $C > 0$ such that

$$\mid \frac{x_{k,m}}{y_{k,m}} - \frac{\bar{x}_k}{\bar{y}_k} \mid \leq \frac{C}{k^2 m^{\alpha_{\min}}}. \tag{253}$$

Hence

$$s_m \leq \frac{C}{m^{\alpha_{\min}}} \sum_{k=1}^{m} \frac{1}{k^2}, \tag{254}$$

which implies (248), since $\sum_{k=1}^{\infty} \frac{1}{k^2} < \infty$. ■

We now use the above lemma to prove (237).

Note that

$$\begin{aligned} \Delta G_1^m(s) &\triangleq \mid G_1(s) - G_1^m(s) \mid, \\ &= \frac{1}{d_x} \left| \sum_{k=1}^{m-1} (-1)^k \left(\frac{2\cos(\frac{k\pi(d_x - x^*)}{d_x})}{s - \lambda_{k,0}} - \frac{\alpha_k \cos(\frac{(d_x - x_{i_m})k\pi}{d_x})}{s - \lambda_{k,0}^{m,n}} \right) \right. \\ &\quad + \left. \sum_{k=m}^{\infty} 2 \frac{(-1)^k \cos(\frac{k\pi(d_x - x^*)}{d_x})}{s - \lambda_{k,0}} \right| \end{aligned} \tag{255}$$

Since $\alpha_k = 2,\ k = 1, 2, \ldots, m-2$ and $\alpha_{m-1} = 1$, see (236), the expression (255) can be re-written as

$$\begin{aligned}
\Delta G_1^m(s) \;&=\; \frac{1}{d_x}\left|\sum_{k=1}^{m-2}(-1)^k\left(\frac{2\cos(\frac{k\pi(d_x-x^*)}{d_x})}{s-\lambda_{k,0}} - \frac{2\cos(\frac{(d_x-x_{i_m})k\pi}{d_x})}{s-\lambda_{k,0}^{m,n}}\right)\right. \\
&\quad +(-1)^{m-1}\left(\frac{\cos(\frac{(m-1)\pi(d_x-x^*)}{d_x})}{s-\lambda_{m-1,0}} - \frac{\cos(\frac{(d_x-x_{i_m})(m-1)\pi}{d_x})}{s-\lambda_{m-1,0}^{m,n}}\right) \\
&\quad \left.+\sum_{k=m-1}^{\infty}\frac{\gamma_k(-1)^k\cos(\frac{k\pi(d_x-x^*)}{d_x})}{s-\lambda_{k,0}}\right| \qquad (256)
\end{aligned}$$

where $\gamma_{m-1} \triangleq 1$ and $\gamma_k \triangleq 2,\ k = m, m+1, \ldots$.

Using the triangle inequality twice on (256), we get

$$\begin{aligned}
\Delta G_1^m(s) \;&\leq\; \frac{2}{d_x}\sum_{k=0}^{m-1}\left|\frac{\cos(\frac{k\pi(d_x-x^*)}{d_x})}{s-\lambda_{k,0}} - \frac{\cos(\frac{k\pi(d_x-x_{i_m})}{d_x})}{s-\lambda_{k,0}^{m,n}}\right| \\
&\quad +\frac{1}{d_x}\left|\frac{\cos(\frac{(m-1)\pi(d_x-x^*)}{d_x})}{s-\lambda_{m-1,0}} - \frac{\cos(\frac{(d_x-x_{i_m})(m-1)\pi}{d_x})}{s-\lambda_{m-1,0}^{m,n}}\right| \\
&\quad +\frac{1}{d_x}\sum_{k=m-1}^{\infty}\left|\frac{\gamma_k\cos(\frac{k\pi(d_x-x^*)}{d_x})}{s-\lambda_{k,0}}\right| \qquad (257)
\end{aligned}$$

Note that the third term in the in the right hand side (RHS) of the inequality (257) converges to zero as it is the tail of a convergent series. To show the convergence of the first and the second terms in (RHS), we set

$$\begin{aligned}
b &\triangleq s & (258)\\
x_{k,m} &\triangleq (-1)^k\cos(\frac{k\pi(d_x-x_{i_m})}{d_x}) & (259)\\
\bar{x}_k &\triangleq (-1)^k\cos(\frac{k\pi(d_x-x^*)}{d_x}) & (260)\\
y_{k,m} &\triangleq s-\lambda_{k,0}^{m,n} & (261)\\
\bar{y}_k &\triangleq s-\lambda_{k,0} & (262)\\
c_{k,m} &\triangleq \frac{\pi^2}{d_x^2}k^2\left[\frac{\sin(\frac{\pi k}{2(m-1)})}{\frac{\pi k}{2(m-1)}}\right]^2 & (263)
\end{aligned}$$

and

$$\bar{c}_k \triangleq \frac{\pi^2}{d_x^2}k^2, \qquad (264)$$

where

$$\lambda_{k,0}^{m,n} = k^2 c_{k,m} \tag{265}$$

and

$$\lambda_{k,0}^{m,n} = k^2 \bar{c}_k, \tag{266}$$

and use Lemma 4. ∎

References

[1] D. V. Widder. *The Heat Equation.* Academic Press, New York, 1975.

[2] A. B. Gumel, W. T. Ang and E. H. Twizell. Efficient parallel algorithm for the two-dimensional diffusion equation subject to specification of mass. *International Journal of Computer Math.*, 1997. Vol. 64, pp. 153-163.

[3] A. C. Antoulas. Approximation of linear dynamical systems. *Article number 1049 in Encyclopedia of Electrical and Electronics Engineering,* edited by J. G. Webster*, John Wiley and Sons*, 1998.

[4] A. C. Antoulas, J. A. Ball, J. Kang, and J. C. Willems. On the solution of the minimal rational interpolation problem. *Linear Algebra and Its Applications, Special Issue on Matrix Problems,* Vol 137/138, pp 511-573, 1990.

[5] M. J. Balas. Feedback control of linear diffusion processes. *International Journal of Control, Vol 29, Number 3 pp. 523-533*, 1979.

[6] J.J. Bloem. editor. *System Identification Competition.* Joint Research Center, European Commission, Luxembourg, 1996.

[7] H. S. Carlslaw and J. C. Jaeger. *Operational Methods In Applied Mathematics.* Oxford University Press, London, 1947.

[8] G. H.Golub and J. M. Ortega. *Scientific Computing and Differential Equations, An Inroduction to Numerical Methods.* Academic Press, San Diego, 1992.

[9] D. Gottlieb and A.Orzag. *Numerical Analysis of Spectral Methods: Theory and Applications.* SIAM, Philadelphia, 1977.

[10] K. Grimme. Krylov Projection Methods for Model Reduction. Ph. D. Thesis, ECE Dept., U. of Illinois Urbana-Champaign, 1997.

[11] M. J. Balas and C. D. Johnson. Identification of unknown force/moment distributions in nonlinear distributed parameter systems. *Developments in Theoretical and Applied Mechanics*, 1998. Vol. XIX, pp. 172-191.

[12] P. C. Tuan, C. C. Ji, L. W. Fong and W. T. Haung. An input estimation approach to online two dimensional inverse heat conduction problems. *Numerical Heat Transfer, Part B*, 1996. Vol. 29, pp. 345-363.

[13] P. Willmott, S. Howison and J. Dewynne. *The Mathematics of Financial Derivatives, A Student Introduction*. Cambridge University Press, Cambridge, 1999.

[14] R. V: Churchill. *Operational Mathematics*. McGraw-Hill Book Company, New York, 1972.

[15] S. Remle. Modeling and parameter estimation of the diffusion equation. *Licentiate thesis, Department of Information Technology, Uppsala University, Uppsala*, 2000.

[16] M. Renardy and R. C. Rogers. *An Introduction to Partial Differential Equations*. Springer-Verlag, New York, 1993.

[17] T. Söderström and P. Stoica. *System Identification*. Prentice Hall International, Hemel Hempstead, UK, 1989.

[18] J. Villadsen and M. L. Michelsen. *Solution of Differential Equation Models by Polynomial Approximation*. Prentice Hall, Englewood Cliffs, N. J., 1978.

[19] T. Wik and C. Breitholtz. Rational transfer function models for biofilm reactors. *AIChE Journal*, 1998. Vol. 44, No. 12, pp. 2647-2657, December.